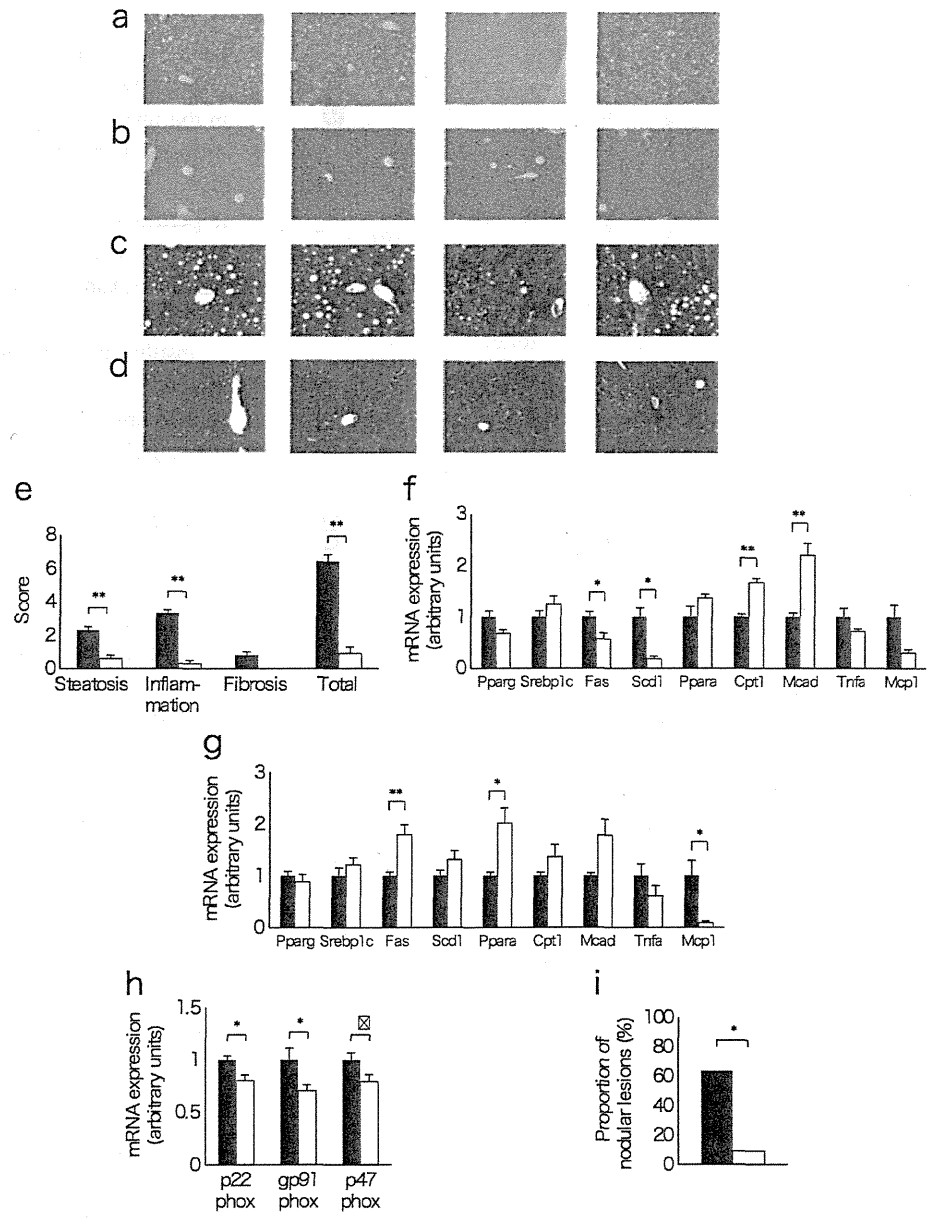

Fig. 7 Effects of a long-term HF diet on the incidence of NASH and liver tumourigenesis in *Irs1*$^{-/-}$ mice. (**a**) Histopathological features of the livers from wild-type and (**b**) *Irs1*$^{-/-}$ mice fed the HF diet for 60 weeks, as assessed using H&E-stained sections (n 4). (**c**) Histopathological features of the livers from wild-type and (**d**) *Irs1*$^{-/-}$ mice fed the HF diet for 60 weeks, as assessed using Masson trichrome-stained sections (n 4). (**e**) NASH/NAFLD Clinical Research Network scoring system definitions and scores [32] for wild-type (black bars) and *Irs1*$^{-/-}$ (white bars) mice fed the HF diet for 60 weeks (n 9). (**f**) mRNA expression of lipogenic and inflammatory cytokine-related genes after 30 and (**g**) 60 weeks on the HF diet, and (**h**) of genes encoding the reduced-form NADPH oxidase complex after 60 weeks on the HF diet in wild-type and *Irs1*$^{-/-}$ mice (n 4–6). (**i**) Proportion of hepatic nodular lesions in wild-type and *Irs1*$^{-/-}$ mice fed the HF diet for 60 weeks (n 11). Values are mean ± SEM; *p<0.05 and **p<0.01; $^{\dagger}p$ 0.05

hypothesis should be further examined using liver-specific *Irs1*$^{-/-}$ and *Irs2*$^{-/-}$ mice [10] in the future.

Another question that remains unclear is whether the contribution or compensation of IRS-2 signalling plays a role in the above-mentioned protective effect. Our data show that *Irs2* expression in *Irs1*$^{-/-}$ mice on the HF diet was significantly higher than in wild-type mice fed the HF diet. However, levels were significantly lower than those in wild-type mice fed the SC diet. Moreover, the basal and insulin-stimulated phosphorylation of Akt in *Irs1*$^{-/-}$ mice on the HF diet was lower than in wild-type mice fed the HF diet (data not shown). These results suggest that IRS-2 may not fully compensate for the loss of IRS-1 in *Irs1*$^{-/-}$ mice on an HF diet. We therefore assumed that the contribution of residual IRS-2 signalling was limited to the livers of *Irs1*$^{-/-}$ mice on the HF diet.

What is the relevance of the present results to the clinical management of humans with diabetes? Therapeutic targeting of IRS-1 may not be advisable, since *IRS1* is an insulin resistance gene in humans [28] and our results suggest that blocking IRS-1-mediated signalling exacerbated glucose tolerance, even though it was able to protect against NASH and liver tumourigenesis. Epidemiological evidence suggests that people with diabetes have significantly higher risks of many forms of cancer [29]. Recently, a meta-analysis of several studies showed that liver cancer is more common in patients with diabetes [30].

Johnson et al commented that the accumulation of experimental and epidemiological evidence is more consistent with the hyperinsulinaemia hypothesis and less so with the hyperglycaemia hypothesis [31] with regard to the increased risk of cancer in patients with diabetes. Here, we showed that the reduction of obesity and hyperinsulinaemia by switching from an HF to an SC diet protected mice against the development of NASH and liver tumourigenesis without changing blood glucose levels. These results support the hyperinsulinaemia hypothesis. How can our results for *Irs1*$^{-/-}$ mice fed an HF diet be explained? We assumed that the protection against NASH and tumour development in *Irs1*$^{-/-}$ mice fed the HF diet was caused by the downregulation of IRS-1-mediated insulin action in the liver, despite systemic hyperinsulinaemia. As described above, the hyperinsulinaemia associated with an HF diet suppresses IRS-2 production, and persistent IRS-1 signalling promotes lipogenesis and hepatic steatosis. Thus, when mice were fed the HF diet, the wild-type mice developed hepatic steatosis, but the *Irs1*$^{-/-}$ mice were protected against the development of NASH and liver tumourigenesis, despite the presence of hyperinsulinaemia. Thus, these results for *Irs1*$^{-/-}$ mice fed an HF diet are consistent with the above-mentioned hyperinsulinaemia hypothesis. Therefore, the prevention of hyperinsulinaemia using glucose-lowering agents such as metformin and thiazolidinedione could not only protect against diabetes, but also against liver tumourigenesis. The effects of metformin on NASH and liver tumourigenesis in this mouse model are now under investigation.

In conclusion, long-term HF diet loading was sufficient to induce NASH and liver tumourigenesis in C57Bl/6J mice. Switching from an HF to an SC diet reduced obesity and insulin resistance, and protected against the development of NASH and liver tumourigenesis in the same mice. Moreover, *Irs1*$^{-/-}$ mice fed an HF diet were dramatically protected against NASH and liver tumourigenesis, suggesting that IRS-1 inhibition might protect against HF diet-induced NASH and liver tumourigenesis, despite the presence of insulin resistance.

Acknowledgements We thank M. Kaji and E. Sakamoto (Department of Endocrinology and Metabolism, Graduate School of Medicine, Yokohama City University, Yokohama, Japan) for their excellent technical assistance and animal care.

Funding This work was supported in part by: Grants-in-Aid for Scientific Research (B) 19390251 and (B) 21390282 from the Ministry of Education, Culture, Sports, Science and Technology (MEXT) of Japan; a Medical Award from the Japan Medical Association; a Grant-in-Aid from the Uehara Memorial Foundation; a Grant-in-Aid from the Daiichi–Sankyo Foundation of Life Science; and a Grant-in-Aid from the Naito Foundation (to Y. Terauchi).

Contribution statement All the authors conceived and designed the study, and participated in the analysis and interpretation of the data. AN drafted the manuscript, and all the other authors revised it critically for intellectual content. All the authors approved the final version of the paper.

Duality of interest The authors declare that there is no duality of interest associated with this manuscript.

References

1. Finucane MM, Stevens GA, Cowan MJ et al (2011) National, regional, and global trends in body-mass index since 1980: systematic analysis of health examination surveys and epidemiological studies with 960 country-years and 9.1 million participants. Lancet 377:557–567
2. Danaei G, Finucane MM, Lu Y et al (2011) National, regional, and global trends in fasting plasma glucose and diabetes prevalence since 1980: systematic analysis of health examination surveys and epidemiological studies with 370 country-years and 2.7 million participants. Lancet 378:31–40
3. Calle EE, Rodriguez C, Walker-Thurmond K, Thun MJ (2003) Overweight, obesity, and mortality from cancer in a prospectively studied cohort of U.S. adults. N Engl J Med 348:1625–1638
4. Inoue M, Iwasaki M, Otani T, Sasazuki S, Noda M, Tsugane S (2006) Diabetes mellitus and the risk of cancer: results from a large-scale population-based cohort study in Japan. Arch Intern Med 166:1871–1877
5. Starley BQ, Calcagno CJ, Harrison SA (2010) Nonalcoholic fatty liver disease and hepatocellular carcinoma: a weighty connection. Hepatology 51:1820–1832
6. Hill-Baskin AE, Markiewski MM, Buchner DA et al (2009) Diet-induced hepatocellular carcinoma in genetically predisposed mice. Hum Mol Genet 18:2975–2988
7. VanSaun MN, Lee IK, Washington MK, Matrisian L, Gorden DL (2009) High fat diet induced hepatic steatosis establishes a permissive microenvironment for colorectal metastases and promotes primary dysplasia in a murine model. Am J Pathol 175:355–364
8. Park EJ, Lee JH, Yu GY et al (2010) Dietary and genetic obesity promote liver inflammation and tumorigenesis by enhancing IL-6 and TNF expression. Cell 140:197–208
9. Saltiel AR, Kahn CR (2001) Insulin signalling and the regulation of glucose and lipid metabolism. Nature 414:799–806
10. Kubota N, Kubota T, Itoh S et al (2008) Dynamic functional relay between insulin receptor substrate 1 and 2 in hepatic insulin signaling during fasting and feeding. Cell Metab 8:49–64
11. Guo S, Copps KD, Dong X et al (2009) The Irs1 branch of the insulin signaling cascade plays a dominant role in hepatic nutrient homeostasis. Mol Cell Biol 29:5070–5083
12. Monetti M, Levin MC, Watt MJ et al (2007) Dissociation of hepatic steatosis and insulin resistance in mice overexpressing DGAT in the liver. Cell Metab 6:69–78
13. Chattopadhyay M, Selinger ES, Ballou LM, Lin RZ (2011) Ablation of PI3K p110-α prevents high-fat diet-induced liver steatosis. Diabetes 60:1483–1492
14. Horie Y, Suzuki A, Kataoka E et al (2004) Hepatocyte-specific Pten deficiency results in steatohepatitis and hepatocellular carcinomas. J Clin Invest 113:1774–1783
15. Kudo Y, Tanaka Y, Tateishi K et al (2011) Altered composition of fatty acids exacerbates hepatotumorigenesis during activation of the phosphatidylinositol 3-kinase pathway. J Hepatol 55:1400–1408
16. Kubota N, Tobe K, Terauchi Y et al (2000) Disruption of insulin receptor substrate-2 causes type 2 diabetes due to liver insulin resistance and lack of compensatory beta-cell hyperplasia. Diabetes 49:1880–1889
17. Terauchi Y, Matsui J, Kamon J et al (2004) Increased serum leptin protects from adiposity despite the increased glucose uptake in white adipose tissue in mice lacking p85alpha phosphoinositide 3-kinase. Diabetes 53:2261–2270

18. Kubota N, Yano W, Kubota T et al (2007) Adiponectin stimulates AMP-activated protein kinase in the hypothalamus and increases food intake. Cell Metab 6:55–68
19. Tamemoto H, Kadowaki T, Tobe K et al (1994) Insulin resistance and growth retardation in mice lacking insulin receptor substrate-1. Nature 372:182–186
20. Araki E, Lipes MA, Patti ME et al (1994) Alternative pathway of insulin signalling in mice with targeted disruption of the IRS-1 gene. Nature 372:186–190
21. Terauchi Y, Iwamoto K, Tamemoto H et al (1997) Development of non-insulin-dependent diabetes mellitus in the double knockout mice with disruption of insulin receptor substrate-1 and beta cell glucokinase genes. Genetic reconstitution of diabetes as a polygenic disease. J Clin Invest 99:861–866
22. Brown MS, Goldstein JL (2008) Selective versus total insulin resistance: a pathogenic paradox. Cell Metab 7:95–96
23. Semple RK, Sleigh A, Murgatroyd PR et al (2009) Postreceptor insulin resistance contributes to human dyslipidemia and hepatic steatosis. J Clin Invest 119:315–322
24. Biddinger SB, Hernandez-Ono A, Rask-Madsen C et al (2008) Hepatic insulin resistance is sufficient to produce dyslipidemia and susceptibility to atherosclerosis. Cell Metab 7:125–134
25. Zhang J, Ou J, Bashmakov Y, Horton JD, Brown MS, Goldstein JL (2001) Insulin inhibits transcription of IRS-2 gene in rat liver through an insulin response element (IRE) that resembles IREs of other insulin-repressed genes. Proc Natl Acad Sci USA 98:3756–3761
26. Leavens KF, Easton RM, Shulman GI, Previs SF, Birnbaum MJ (2009) Akt2 is required for hepatic lipid accumulation in models of insulin resistance. Cell Metab 10:405–418
27. Kadowaki T, Ueki K, Yamauchi T, Kubota N (2012) SnapShot: insulin signaling pathways Cell 148:624 (Abstract)
28. Rung J, Cauchi S, Albrechtsen A et al (2009) Genetic variant near IRS1 is associated with type 2 diabetes, insulin resistance and hyperinsulinemia. Nat Genet 41:1110–1115
29. Giovannucci E, Harlan DM, Archer MC et al (2010) Diabetes and cancer: a consensus report. Diabetes Care 33:1674–1685
30. Vigneri P, Frasca F, Sciacca L, Pandini G, Vigneri R (2009) Diabetes and cancer. Endocr Relat Cancer 16:1103–1123
31. Johnson JA, Pollak M (2010) Insulin, glucose and the increased risk of cancer in patients with type 2 diabetes. Diabetologia 53:2086–2088
32. Kleiner DE, Brunt EM, Van Natta M et al (2005) Design and validation of a histological scoring system for nonalcoholic fatty liver disease. Hepatology 41:1313–1321

Diabetologia (2012) 55:3318–3330
DOI 10.1007/s00125-012-2711-1

ARTICLE

Depletion of homeodomain-interacting protein kinase 3 impairs insulin secretion and glucose tolerance in mice

N. Shojima · K. Hara · H. Fujita · M. Horikoshi · N. Takahashi · I. Takamoto · M. Ohsugi · H. Aburatani · M. Noda · N. Kubota · T. Yamauchi · K. Ueki · T. Kadowaki

Received: 5 June 2012 / Accepted: 7 August 2012 / Published online: 16 September 2012

Abstract
Aims/hypothesis Insufficient insulin secretion and reduced pancreatic beta cell mass are hallmarks of type 2 diabetes. Here, we focused on a family of serine-threonine kinases known as homeodomain-interacting protein kinases (HIPKs). HIPKs are implicated in the modulation of Wnt signalling, which plays a crucial role in transcriptional activity, and in pancreas development and maintenance. The aim of the present study was to characterise the role of HIPKs in glucose metabolism.
Methods We used RNA interference to characterise the role of HIPKs in regulating insulin secretion and transcription activity. We conducted RT-PCR and western blot analyses to analyse the expression and abundance of HIPK genes and proteins in the islets of high-fat diet-fed mice. Glucose-induced insulin secretion and beta cell proliferation were measured in islets from *Hipk3*$^{-/-}$ mice, which have impaired glucose tolerance owing to an insulin secretion deficiency. The abundance of pancreatic duodenal homeobox (PDX)-1 and glycogen synthase kinase (GSK)-3β phosphorylation in *Hipk3*$^{-/-}$ islets was determined by immunohistology and western blot analyses.
Results We found that HIPKs regulate insulin secretion and transcription activity. *Hipk3* expression was most significantly increased in the islets of high-fat diet-fed mice. Furthermore, glucose-induced insulin secretion and beta cell proliferation were decreased in the islets of *Hipk3*$^{-/-}$ mice. Levels of PDX1 and GSK-3β phosphorylation were significantly decreased in *Hipk3*$^{-/-}$ islets.
Conclusions/interpretation Depletion of HIPK3 impairs insulin secretion and glucose tolerance. Decreased levels of HIPK3 may play a substantial role in the pathogenesis of type 2 diabetes.

Keywords Glucose homeostasis · Homeodomain-interacting protein kinase · Insulin secretion

Abbreviations

ChIP	Chromatin immunoprecipitation
GSK	Glycogen synthase kinase
HIPK	Homeodomain-interacting protein kinase
NK	Neurokinin
PCNA	Proliferating cell nuclear antigen
PDX	Pancreatic duodenal homeobox
SF-1	Splicing factor 1
siRNA	Small interfering RNA

Introduction

Type 2 diabetes is a complex disease characterised by chronic hyperglycaemia resulting from insulin resistance

Electronic supplementary material The online version of this article (doi:10.1007/s00125-012-2711-1) contains peer-reviewed but unedited supplementary material, which is available to authorised users.

N. Shojima · K. Hara (✉) · H. Fujita · M. Horikoshi · N. Takahashi · I. Takamoto · M. Ohsugi · N. Kubota · T. Yamauchi · K. Ueki · T. Kadowaki (✉)
Department of Diabetes and Metabolic Disease, Graduate School of Medicine, University of Tokyo, 113-8655 Hongo 7-3-1, Bunkyo-ku, Tokyo, Japan
e-mail: thara-tky@umin.ac.jp
e-mail: kadowaki-3im@h.u-tokyo.ac.jp

N. Takahashi
Center for Disease Biology and Integrative Medicine, Faculty of Medicine, University of Tokyo, Tokyo, Japan

H. Aburatani
Research Center for Advanced Science and Technology, University of Tokyo, Tokyo, Japan

M. Noda
National Center for Global Health and Medicine, Tokyo, Japan

and impaired beta cell function [1–3]. Accumulating evidence shows that Wnt signalling modulates beta cell function [4–9]. The Wnts are a family of secreted glycoproteins that influence cell development via autocrine and paracrine mechanisms [10, 11]. Activation of the canonical pathway occurs by binding of Wnt ligands to the frizzled receptor. This binding triggers an intracellular signalling cascade, which leads to serine/threonine phosphorylation, inactivation of glycogen synthase kinase (GSK)-3β and destabilisation of the destruction complex, preventing GSK3β phosphorylation of β-catenin. This mechanism enables the accumulation and nuclear translocation of β-catenin. Once inside the nucleus, β-catenin acts in combination with the T cell factor to stimulate transcription of Wnt-responsive genes.

GSK-3 was originally identified as a serine/threonine kinase that inactivates glycogen synthase. GSK3 affects many cellular processes, including transcription, cell cycle regulation and apoptosis. GSK3β has been shown to affect beta cell mass, proliferation and apoptosis [12–14].

Homeodomain-interacting protein kinases (HIPKs) are implicated in the modulation of Wnt signalling in cultured cells [15], and in mouse [16, 17], *Drosophila* [18, 19] and *Xenopus* embryos [20, 21]. Members of the HIPK family (HIPK1, HIPK2, HIPK3, HIPK4) were originally identified as binding partners of the neurokinin (NK) homeodomain protein [22]. HIPKs have been reported to be essential for coordinated death in early developmental stages and for the regulation of proper cell number in diverse tissue types. Studies have shown that the HIPK family, and in particular its most studied member, HIPK2, interact with, phosphorylate and modulate the function of other homeodomain proteins, as well as other transcription factors, including p53 [23–25] and carboxy-terminal binding protein (CtBP)-1 [26, 27]. HIPK2 has been reported to modulate the transcriptional activity of pancreatic duodenal homeobox (PDX)-1 [28], which plays a crucial role in pancreas development [29–31].

Several studies have revealed important roles of HIPK3 in the regulation of transcription and phosphorylation in cultured cells [32–36]. HIPK3 overproduction has been reported to enhance androgen receptor-dependent transcription in various cell lines [32]. HIPK3 induced Fas-associated death domain (FADD) phosphorylation and inhibited Fas-mediated Jun NH2-terminal kinase activation [33]. HIPK3 also increased splicing factor 1 (SF-1) activity for steroidogenic gene transcription in response to cAMP through phosphorylation of death-associated protein 6 [35]. Interestingly, *HIPK1*, *HIPK2* and *HIPK3* expression in islets from patients with type 2 diabetes is decreased by 32% (p=0.326), 30% (p=0.082) and 46% (p=0.064), respectively, according to data from the Diabetes Genomic Anatomic Project [3], suggesting that HIPK genes play a role in the control of beta cell function. However, the question of whether HIPKs might be involved in the effects of glucose metabolism has not been addressed.

The current study was undertaken to define the mechanisms by which HIPKs regulate glucose metabolism. Here we show that *Hipk* transcripts are expressed in pancreatic beta cells, and modulate insulin secretion and insulin promoter activity. We found that a high-fat diet enhanced *Hipk3* expression. Moreover, our analysis of *Hipk3*$^{-/-}$ mice revealed that they had impaired glucose tolerance due to a deficiency of insulin secretion. We also demonstrated that levels of PDX1 and phosphorylation of GSK3β were significantly decreased in *Hipk3*$^{-/-}$ islets. Hence, our data provide evidence of a new mechanism by which insulin secretion is regulated.

Methods

RT-PCR Total RNA was isolated from mouse islets and mouse pancreas using TRIzol reagent (Invitrogen, Carlsbad, CA, USA). RT-PCR was performed using reverse transcriptase (RevTraAce; Toyobo, Osaka, Japan). The RT-PCR products were amplified using ExTaq polymerase (Takara, Kyoto, Japan). The gene-specific primer pairs were used, as previously described [37].

Quantitative RT-PCR Quantification of the selected genes was performed using TaqMan gene expression assays with a commercially available system (7900HT; Applied Biosystems, Foster City, CA, USA). For each gene, an assay was selected to amplify the region corresponding to the location of the relevant probe. Gene expression analysis was performed using commercially available mouse assays as follows: *Hipk1*: Mm00501689_m1; *Hipk2*: Mm00439329_m1; *Hipk3*: Mm00468880_m1; *Pdx1*: Mm00435565_m1; *Gck*: Mm00439129_m1; *Slc2a2*: Mm00446229_m1; Cyclin D1: Mm00432359_m1; *Hnf4* (also known as *Hnf4a*): m00433964_m1; *Tcf7l2*: Mm00501505_m1; *Irs2*: Mm03038438_m1; *Ins1*: Mm01950294_s1; *Ins2*: Mm00731595_g1; *Hnf1a*: Mm00493434_m1; *Hnf1b*: Mm00447459_m1; *Irs1*: Mm01278327_m1; *Ucp2*: Mm00627599_m1; and *Gapdh*: Mm99999915_g1 (Applied Biosystems). The assays for *Gapdh* and *Pdx1* were performed in parallel as controls. Standard TaqMan cycling conditions were used and all reactions were performed in triplicate. Changes in expression levels in quantitative PCR were calculated as $2^{-\Delta\Delta C_t}$ (cycle threshold) values and presented relative to average changes.

Immunoprecipitation and immunoblotting analysis of mouse islets Polyclonal anti-PDX1, anti-hepatocyte nuclear factor 4 alpha, anti-GSK3β, anti-phospho-GSK3β(Ser9), anti-β-catenin and anti-α-tubulin antibodies were purchased from Santa Cruz Biotechnology (Santa Cruz, CA, USA). Polyclonal anti-IRS2 antibodies were purchased from Cell Signaling Technology (Beverly, MA, USA). Islets were sonicated, using

an ultrasound sonicator, in 300 to 500 μl ice-cold buffer containing: 0.5% (vol./vol.) Triton X-100, 50 mmol/l TRIS-HCl (pH 8.0), 100 mmol/l NaCl, 1 mmol/l EDTA, 1 mmol/l Na_3VO_4, 10 mmol/l NaF and 1 mmol/l phenylmethylsulfonyl fluoride. Supernatant fractions were cleared at 12,000*g* for 5 min, and incubated with protein A-Sepharose and each specific antibody. Samples were separated by SDS-polyacrylamide gel electrophoresis and immunodetection performed with a kit (ECL; Amersham Bioscience, Arlington Heights, IL, USA). Protein was prepared from more than 100 islets pooled from several mice of identical genotype.

RNA interference and transient transfection Small interfering RNA (siRNA)-Lipofectamine 2000 complexes were prepared using 50 nmol/l siRNA for Hipk genes (Stealth Select RNAi; Invitrogen) and control siRNA (Invitrogen). Islets were precultured for 24 h, medium was changed to OptiMEM (Invitrogen) and siRNA-Lipofectamine 2000 complexes with or without DNA-Lipofectamine 2000 complexes were added. After 8 h incubation, the transfection medium was aspirated and replaced, for an additional 48 h, with fresh culture medium containing 2.8 mmol/l glucose.

Luciferase assays Insulin reporter constructs were constructed from rat pancreas cDNA and genomic DNA using Advantage2 Taq (Invitrogen). The luciferase reporter plasmid harbouring the 5′-flanking region of rat *Ins1* exon 1 (□450 to 51) was subcloned into the pGL4 vector (Promega Biosciences, Madison, WI, USA). Islets plated on to a 24 well plate were transfected with 0.5 μg of each luciferase reporter plasmid and 0.02 μg Renilla luciferase plasmid with the herpes simplex virus thymidine kinase promoter (phRL-TK) using Lipofectamine 2000. Cells were collected 48 h after transfection and luciferase assays were carried out (Promega).

Chromatin immunoprecipitation assay Assays were performed in mouse islets. A chromatin immunoprecipitation (ChIP) assay kit (Upstate, Lake Placid, NY, USA) was used according to procedures suggested by the manufacturer. After crossing and sonication, cell lysates were immunoprecipitated with the indicated antibodies. The eluted genomic DNA from immunoprecipitates was subjected to PCR amplification. Anti-HIPK1, anti-HIPK2, anti-HIPK3 and anti-PDX1 antibodies, as well as control rabbit IgG (Santa Cruz Biotechnology) were used in ChIP assays. For PCR primer sequences, see electronic supplementary material (ESM) Table 1.

Analysis of Hipk3$^{-/-}$ mice Mice deficient for *Hipk3* were generated using the gene trapping method developed by Lexicon Genetics (Woodlands, TX, USA) and supplied by CLEA (Tokyo, Japan). The artificial DNA was designed such that it could be inserted randomly into any gene, preventing the RNA splicing mechanism from working properly and thereby knocking out the gene's function. The inserted DNA was specifically engineered to disrupt the function of the trapped gene, activate a selectable marker, enable the generation of knockout mice and allow precise identification of the chromosomal insertion site (www.lexpharma.com/research/drug-discovery/gene-knockouts.html, last accessed 8 August 2012). Mice were 8 to 20 weeks of age at the time of the experiment. Male 8-week-old BKS. Cg-+*Lepr^{db}*/+*Lepr^{db}*/Jcl (*db/db*) mice and BKS. Cg-*m*+/*m*+/Jcl mice (control) were purchased (CLEA). We used a high-fat diet consisting of 32% fat, 25.5% (wt/wt) protein, 2.9% fibre, 4.0% ash, 29.4% carbohydrates and 6.2% water (CLEA). For all other experiments, the diet consisted of standard chow (CLEA) with the following composition: 25.6% (wt/wt) protein, 3.8% fibre, 6.9% ash, 50.5% carbohydrates, 4% fat and 9.2% water.

Mice were fasted for >16 h before the glucose tolerance test, then loaded with 1.5 mg/g body weight glucose by oral or intraperitoneal administration. Blood samples were collected from the orbital sinus at various time points and glucose measured using an automatic blood glucose meter (Glutest Ace; Sanwa Kagaku, Nagoya, Japan). Insulin and GLP-1 levels were determined using a mouse insulin ELISA kit (Shibayagi, Shibukawa, Japan) and GLP-1 ELISA kit (Wako, Osaka, Japan), respectively. Mice were intraperitoneally challenged with 0.75 mU/g body weight human insulin (Novolin R; Novo Nordisk, Bagsvaerd, Denmark) in an insulin tolerance test. Animal care and the procedures of the experiments were approved by the Animal Care Committee of the University of Tokyo.

Histological and immunohistochemical analysis of mouse islets Female mice (n=4) aged 8 to 20 weeks were used for each genotype and 20 sections of islets were evaluated for morphometry. We studied four animals each per genotype and diet. Analysis was based on cell counts ranging from 1,500 to 2,000 per control and transgenic mouse islet samples. Tissues were routinely processed for paraffin embedding, and 4 μm sections were cut and mounted on silanised slides. Pancreatic sections were stained with anti-insulin, anti-HIPK3 anti-proliferating cell nuclear antigen (PCNA), anti-PDX1 and anti-phspho-GSK3β antibodies. Non-specific staining was blocked by 2 mg/ml poly-L-lysine pre-absorption [38]. Images of pancreatic tissue and islet beta cells were viewed on the monitor of a computer through a microscope connected to a charge-coupled device camera (Olympus, Tokyo, Japan). The areas of the pancreas, beta cells and non-beta cells were traced manually and analysed with Win ROOF software (Mitani, Fukui, Japan).

Islet isolation and culture Mouse pancreas was incubated for 30 min at 37°C in 2.5 ml KRB buffer containing collagenase

(Sigma-Aldrich, St Louis, MO, USA). The pancreas was dispersed by pipetting and washed twice with KRB buffer. Mouse recombinant Wnt3a was purchased from Wako. Glibenclamide, LiCl and 1-azakenpaullone were purchased form Sigma-Aldrich. Static incubation was performed for 1 h at 37°C with ten islets per tube after 20 min of preincubation. Insulin levels were determined with a mouse insulin ELISA kit (Shibayagi). For the perifusion experiment, ten islets of similar size were maintained in KRB buffer delivered using a peristaltic pump. Perifusion was as follows: 30 min with KRB buffer containing 2.8 mmol/l glucose; 20 min with KRB buffer containing 20 mmol/l glucose; 40 min with KRB buffer containing 2.8 mmol/l glucose; 10 min with KRB buffer containing 2.8 mmol/l KCl; and 30 min with KRB buffer containing 2.8 mmol/l glucose. Perifusate was collected every 5 min. At the end of the perifusion, islets were collected by handpicking and extracted with 0.18 mol/l HCl in 70% ethanol for determination of insulin content.

ATP measurement ATP measurement of islets was performed as previously described with some modifications [39]. After preincubation, 1 ml fresh KRB buffer containing 2.8, 10 or 22 mmol/l glucose was introduced. Incubation was carried out for 1 h at 37°C and stopped by adding trichloroacetic acid. ATP content of the cells was assayed in duplicate by the luminometric method using an ATP bioluminescent assay kit (Sigma).

Two-photon excitation imaging Two-photon excitation imaging of islets was performed as previously described [40]. Ca^{2+} measurements were performed using fura-2 as the Ca^{2+} indicator. Fura-2 post-stimulation fluorescence (*F*) was normalised to the resting fluorescence (*F0*). The increase of Ca^{2+} concentration was calculated as $(F0-F)/F0$.

Statistical analysis All data are presented as the mean± SEM of independent replicates. All statistical analyses were performed by one-way ANOVA or χ^2 analysis as indicated.

Results

The reduction of Hipk1, Hipk2 and Hipk3 expression by RNA interference attenuates insulin secretion We assessed the expression of Hipk family genes by RT-PCR using cDNA prepared from isolated mouse islets. Hipk family expression was detected in islets (Fig. 1a). Quantitative RT-PCR using TaqMan gene expression assays revealed that the expression of *Hipk2* and *Hipk3* was two- and 2.5-fold higher, respectively, than that of *Hipk1* (Fig. 1b,c). We estimated whether Hipk genes can also decrease insulin secretion from isolated islets. siRNA to *Hipk1*, *Hipk2* and *Hipk3* suppressed endogenous expression by 45%, 44% and 46%, respectively (Fig. 1d), leading upon stimulation with 20 mmol/l glucose to decreases in insulin secretion by 42%, 44% and 46%, respectively (Fig. 1d). We also found that simultaneous inhibition of *Hipk1* and *Hipk2*, *Hipk2* and *Hipk3*, and *Hipk1* and *Hipk3* inhibited insulin secretion by 52%, 54% and 56%, respectively (Fig. 1e). Simultaneous inhibition of *Hipk1*, *Hipk2* and *Hipk3* inhibited insulin secretion by 78% (Fig. 1e). These observations suggest that the additive inhibition of Hipk genes leads to impaired beta cell function. To evaluate whether Hipk genes also affect insulin promoter transcriptional activity, we conducted luciferase assays using RNA interference approaches. siRNA to *Hipk1*, *Hipk2* and *Hipk3* decreased insulin promoter transcriptional activity in isolated mouse islets by 38%, 44% and 52%, respectively (Fig. 1f). Endogenous insulin transcript levels were assessed by quantitative RT-PCR and correlated with the results obtained in luciferase reporter assays (Fig. 1g). ChIP assay revealed that HIPKs interacted with the insulin promoter (Fig. 1h).

Hipk family expression in the islets of mice fed a high-fat diet mRNA expression of *Hipk1*, *Hipk2*, and *Hipk3* was increased in the extracts of islets isolated from B6 mice fed a high-fat diet for 12 weeks, compared with islets from control chow-fed B6 mice. Increases were by 44%, 78% and 109%, respectively (Fig. 2a). HIPK1, HIPK2 and HIPK3 levels were increased by 41%, 98% and 112%, respectively, in the extracts of islets isolated from B6 mice fed a high-fat diet (Fig. 2b), indicating that HIPK3 accumulation may correlate with glucose tolerance in this environmental model of type 2 diabetes.

Hipk3 expression is enhanced in the islets of db/db mice We examined *Hipk3* expression in *db/db* mice. *Hipk3* mRNA was increased by 96% and 54%, respectively, in the extracts of islets isolated from 8- and 20-week-old *db/db* mice compared with 8-week-old control mouse islets (Fig. 2c). HIPK3 protein was increased by 94% and 51%, respectively, in the extracts of islets isolated from 8- and 20-week-old *db/db* mice compared with 8-week-old control mouse islets (Fig. 2d). We also performed immunohistochemical analysis, finding that HIPK3 levels were increased in islets from *db/db* mice (Fig. 2e). This indicates that HIPK3 accumulation correlates with glucose tolerance in this genetic model of type 2 diabetes.

$Hipk3^{-/-}$ mice had impaired insulin secretion To elucidate the physiological role of HIPK3 in glucose metabolism, we examined the phenotypes of $Hipk3^{-/-}$ mice. $Hipk3^{\square/\square}$ mice showed normal weight gain on a standard and a high-fat diet (Fig. 3a). Their overall appearance at death after 12 weeks on a high-fat diet revealed no difference between $Hipk3^{\square/\square}$ and wild-type mice on either a standard or a high-fat diet. We performed the OGTT on mice fed a standard diet. $Hipk3^{\square/\square}$ mice fed a standard diet had significantly impaired

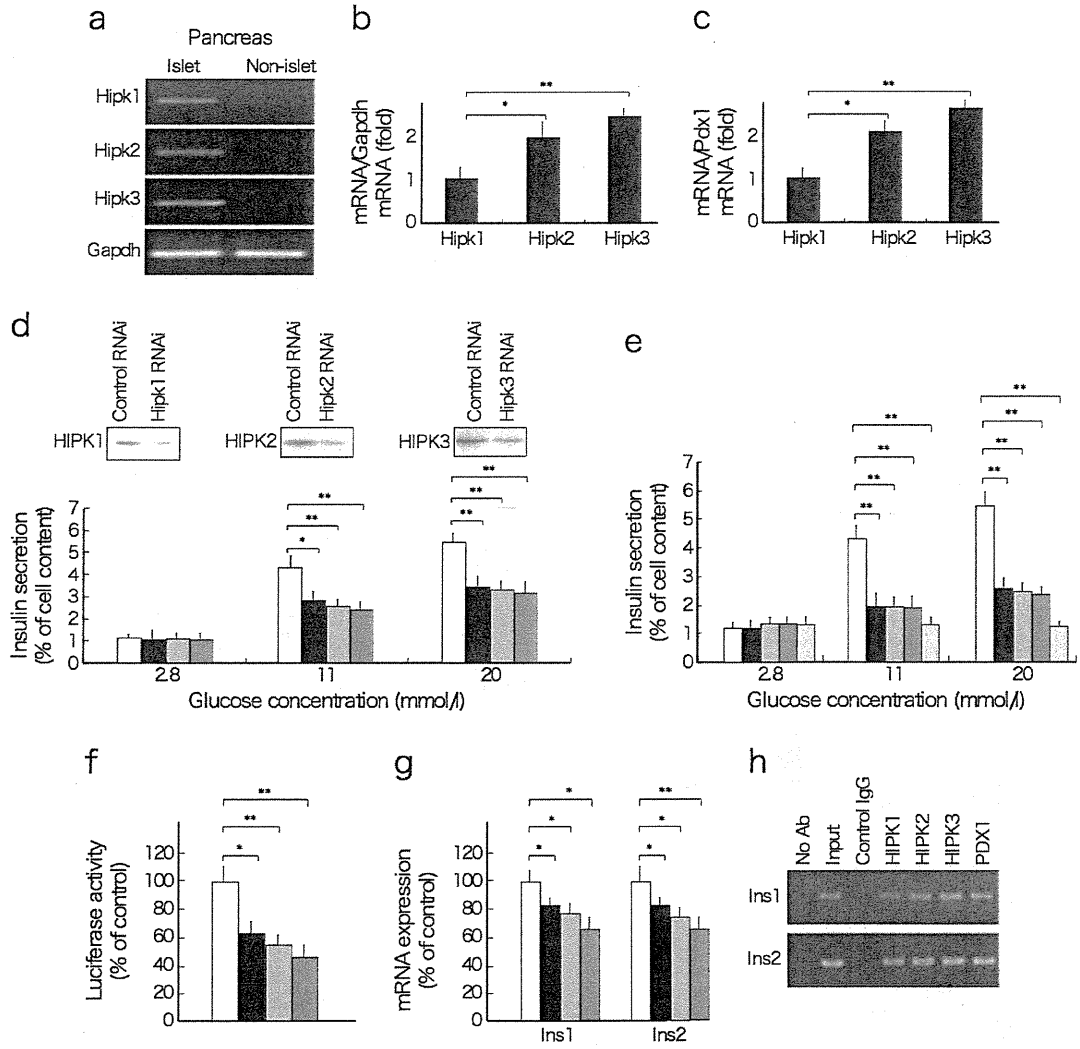

Fig. 1 (**a**) RT-PCR analysis of Hipk genes in islets isolated from a wild-type mouse. Quantitative RT-PCR using TaqMan gene expression assays was performed to validate the relative expression of Hipk genes. (**b**) Assays for *Gapdh* and (**c**) *Pdx1* were performed in parallel as control. (**d**) Blots showing *Hipk1*, *Hipk2* and *Hipk3* inactivation by RNA interference (RNAi). siRNA-Lipofectamine 2000 complexes were prepared (n=4), and suppression of glucose-stimulated insulin secretion by gene inactivation was quantified. White bars, control; black bars, *Hipk1*; light grey bars, *Hipk2*; dark grey bars, *Hipk3*. (**e**) Glucose-stimulated insulin secretion was decreased by a combination of *Hipk1*, *Hipk2* and *Hipk3* RNA interference treatment (n=4). White bars, control; black bars, *Hipk1*+*Hipk2*; mid-grey bars, *Hipk2*+*Hipk3*; dark grey bars, *Hipk1*+*Hipk3*; light grey bars, *Hipk1*+*Hipk2*+*Hipk3*. (**f**) Insulin promoter transcriptional activity was suppressed by *Hipk1*, *Hipk2* and *Hipk3* inactivation by RNA interference in mouse isolated islets. Islets were precultured for 24 h, and DNA-Lipofectamine 2000 complexes along with siRNA-Lipofectamine 2000 complexes were added (n=4). Isolated islets were transfected with 0.1 μg of the rat insulin I promoter luciferase reporter plasmid pINS (□450 to 51)-pGL4 and by siRNA to *Hipk1*, *Hipk2* and *Hipk3*, and control siRNA. Luciferase activity was measured 48 h after transfection. Key as above (**d**). (**g**) Endogenous insulin transcript levels were assessed by quantitative RT-PCR. Key as in (**d**). (**h**) The recruitment of HIPKs on the *Ins1* and *Ins2* promoter in mouse islets. ChIP assays were performed in islets using the indicated antibodies (Ab) and primer pairs. As controls, PCR reactions were performed with input DNA (lane 2), DNA immunoprecipitated by rabbit IgG (lane 3) and DNA that was immunoprecipitated in the absence of antibody (lane 1). Data represent the average results from three independent ChIP experiments. Data (**a**–**g**) are from three independent islet preparations and experiments, with measurements in duplicate, and are presented as mean±SEM; *p<0.05 and **p<0.01 compared with control siRNA

glucose tolerance (Fig. 3b) and decreased insulin response to glucose (Fig. 3c) compared with wild-type mice. Under standard diet conditions, intraperitoneal glucose tolerance and glucose-dependent insulin secretion of *Hipk3*$^{□/□}$ mice were similar to those of wild-type mice (Fig. 3b). *Hipk3*$^{□/□}$ mice had significantly impaired GLP-1 secretion during an OGTT compared with that of wild-type mice (Fig. 3d). *Hipk3*$^{□/□}$ mice fed a high-fat diet for 4 and 12 weeks had significantly impaired glucose tolerance (Fig. 3e, f) and decreased insulin response to glucose (Fig. 3g, h, k) compared with wild-type mice. The glucose-lowering effect of insulin did not differ between *Hipk3*$^{□/□}$ and wild-type mice on a standard or a high-fat diet (Fig. 3i, j, l), supporting the hypothesis that glucose intolerance in *Hipk3*$^{-/-}$ mice was

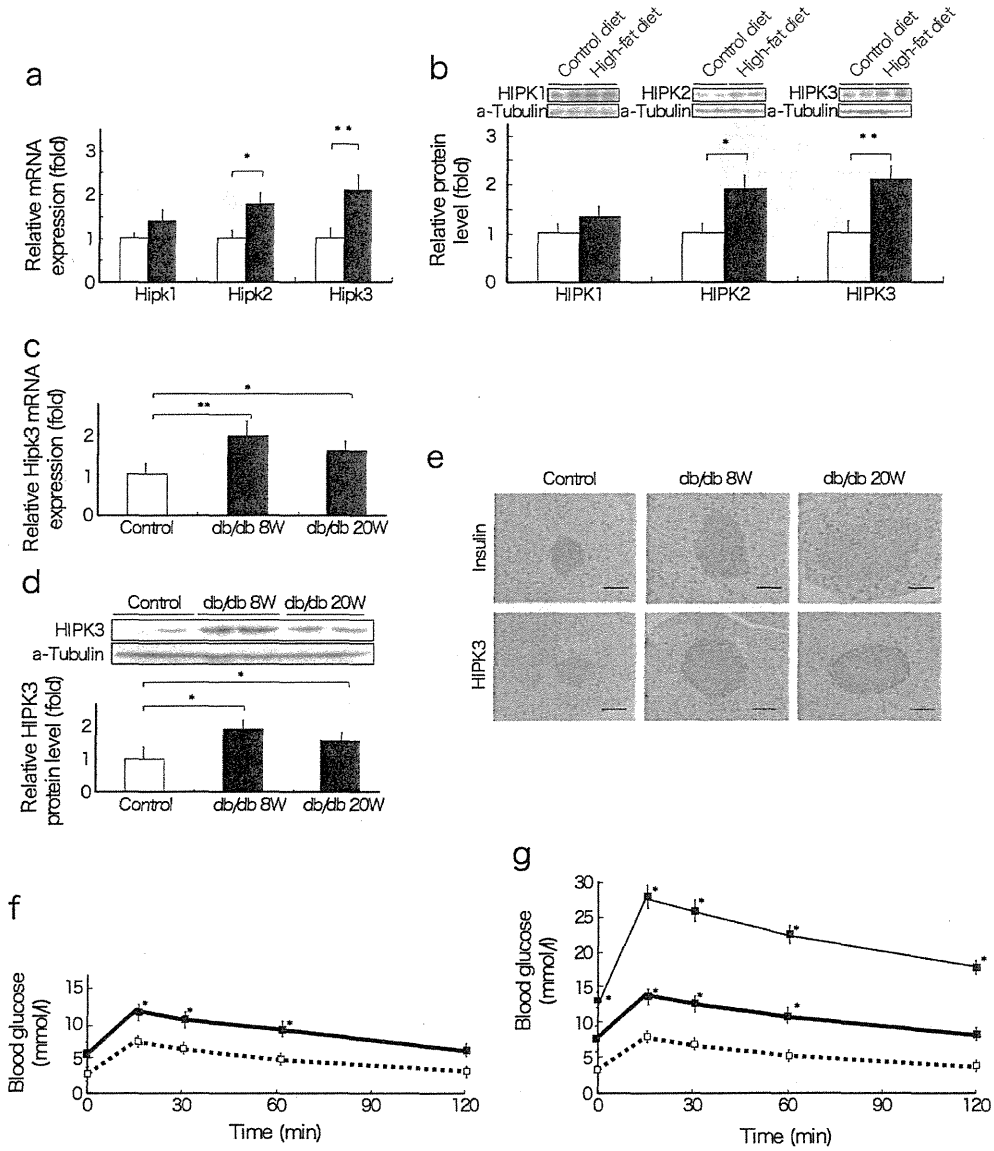

Fig. 2 Changes in Hipk genes mRNA expression (**a**) and protein (**b**) abundance in islets from mice fed a high-fat (black bars; white bars, control) diet (n=4). Quantitative RT-PCR analysis of *Hipk3* was done in islets isolated from wild-type mice. Protein was prepared from more than 100 islets pooled from several mice. Protein samples from lysates of isolated islets were immunoprecipitated using anti-HIPK1, -HIPK2 and -HIPK3 antibodies, and separated by SDS-PAGE. Western blot analyses were performed with the same antibodies. (**c**) Changes to *Hipk3* mRNA expression and (**d**) protein levels in islets from 8-week-old (8W) and 20-week-old (20W) *db/db* mice (n=4). RT-PCR analysis of *Hipk3* was done in islets isolated from wild-type mice. Samples were normalised using α-tubulin. Protein samples from lysates of isolated islets were separated by SDS-PAGE and western blot analyses performed using anti-HIPK3 antibody. (**e**) Immunohistochemical analysis of paraffin-embedded sections from 8- and 20-week-old *db/db* mice using anti-insulin and anti-HIPK3 antibodies. Scale bars, 100 μm. (**f**) OGTT results for mice fed a high-fat diet (continuous black line; dotted line, control diet) and (**g**) for *db/db* mice (dotted line, control; thick black line, *db/db* 8 weeks old; thin black line, *db/db* 20 weeks old). Data represent means±SEM; *p<0.05 and **p<0.01 compared with control

not the result of major differences in insulin responsiveness to glucose.

Loss of Hipk3 decreases glucose-induced insulin secretion We next determined glucose-induced insulin secretion in *Hipk3*$^{\square/\square}$ mice by static incubation of the same numbers of islets. Whereas insulin secretion into the medium by islets from *Hipk3*$^{\square/\square}$ and wild-type mice was similar at 2.8 mmol/l glucose, insulin secretion by islets from *Hipk3*$^{\square/\square}$ mice was significantly decreased at 11 and 20 mmol/l glucose compared with islets from wild-type mice (Fig. 4a). However, the secretory response in *Hipk3*$^{-/-}$ mouse islets was restored by treatment with KCl or glibenclamide (Fig. 4b). To characterise the molecular defect in insulin secretion, we performed pancreas perifusion experiments. In *Hipk3*$^{-/-}$ mice, the insulin secretory response to 20 mmol/l glucose was delayed and decreased

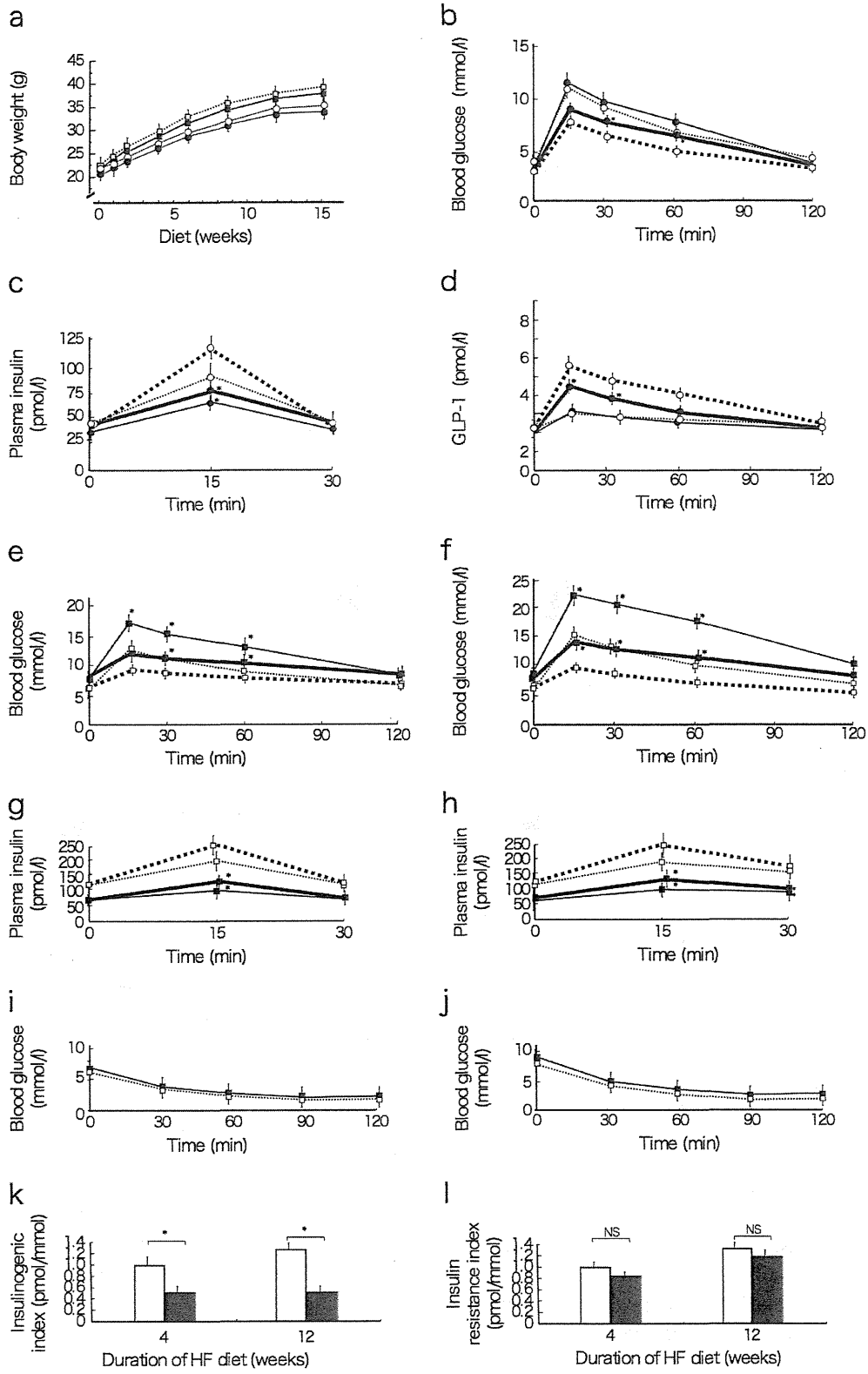

Fig. 3 Impaired glucose homeostasis and insulin secretion in *Hipk3*$^{-/-}$ mice. (**a**) The body weight of *Hipk3*$^{\square/\square}$ mice on a high-fat (black squares) and control (black circles) diet, and of wild-type mice on high-fat (white squares) and control (white circles) diet was similar. (**b**) Mice were loaded with 1.5 mg/g body weight glucose by oral (OGTT) (bold dotted line, wild-type; bold continuous line, *Hipk3*$^{\square/\square}$) or intraperitoneal (IPGTT) (thin dotted line, wild-type; thin continuous line, *Hipk3*$^{\square/\square}$) administration. The OGTT revealed impaired glucose homeostasis in *Hipk3*$^{-/-}$ mice (n=7). (**c**) The OGTT revealed impaired insulin secretion in *Hipk3*$^{-/-}$ mice. Insulin levels were determined using a mouse insulin ELISA kit. (**d**) Impaired GLP-1 secretion in *Hipk3*$^{-/-}$ mice. **e** *Hipk3*$^{\square/\square}$ mice fed a high-fat diet for 4 or (**f**) 12 weeks had significantly impaired glucose tolerance. Key, as above (**b**). (**g**) The glucose intolerance observed in *Hipk3*$^{\square/\square}$ mice fed a high-fat diet for 4 or (**h**) 12 weeks coincided with impaired insulin release. (**i**) The insulin tolerance test showed that wild-type (dotted line) and *Hipk3*$^{\square/\square}$ (continuous line) mice fed a high-fat diet for 4 or (**j**) 12 weeks had similar rates of glucose clearance. (**k**) Insulinogenic index, defined as the ratio of insulin to glucose at 30 min after an oral glucose load in *Hipk3*$^{\square/\square}$ (black bars) and wild-type (white bars) mice on a high-fat (HF) diet. (**l**) Values under the glucose curve and under the insulin curve during the OGTT were similar between *Hipk3*$^{\square/\square}$ and wild-type mice. The insulin resistance index was calculated as AUC of insulin/AUC of glucose in the OGTT. Data represent means±SEM; *p<0.05 compared with wild-type control mice

(Fig. 4c). The ATP content was significantly decreased in *Hipk3*$^{-/-}$ islets (Fig. 4d). The increase in intracellular calcium concentration in response to glucose was impaired in islets of *Hipk3*$^{-/-}$ mice (Fig. 4e).

Loss of Hipk3 decreases beta cell proliferation and increases apoptosis Although the insulin content of islets from *Hipk3*$^{\square/\square}$ mice was not decreased at week 4 of a high-fat diet, it was significantly decreased at week 12 of a high-

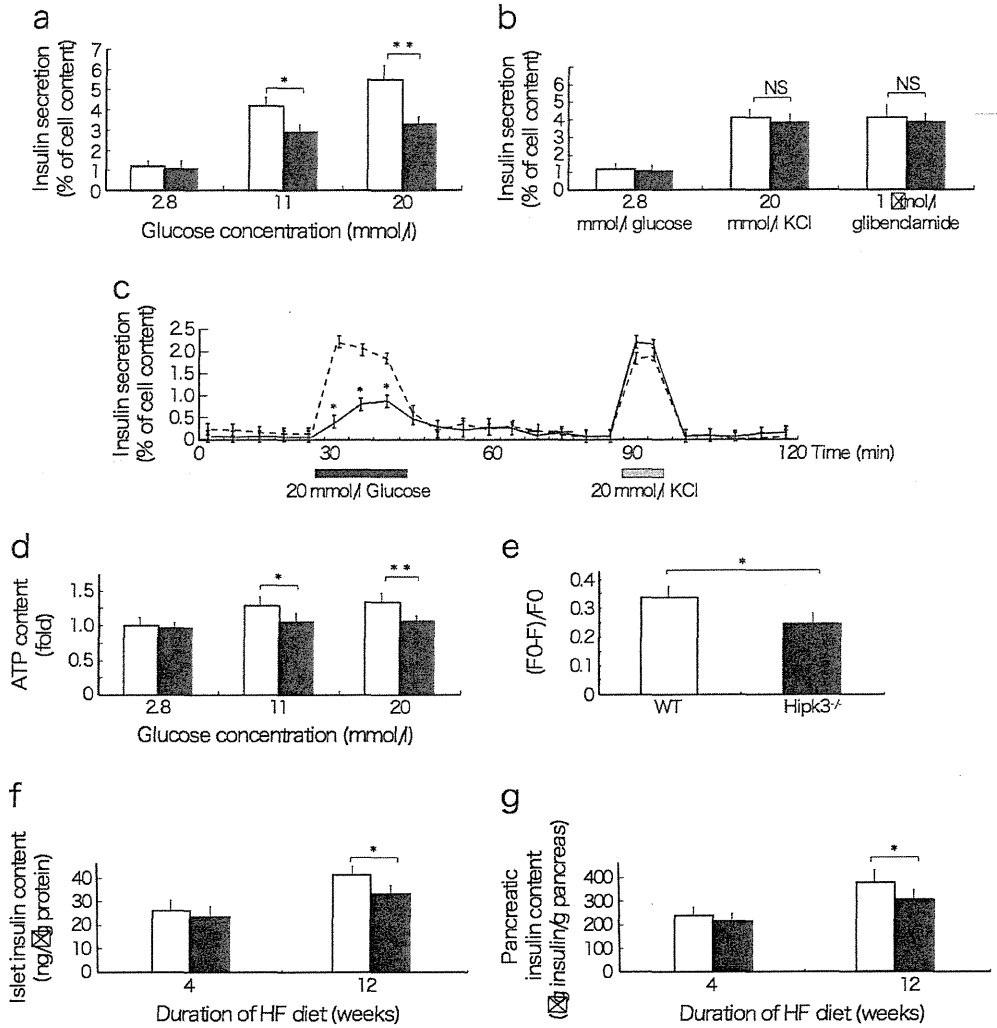

Fig. 4 Characteristics of islets from *Hipk3*$^{\square/\square}$ mice. (**a**) Insulin secretion by islets from *Hipk3*$^{\square/\square}$ mice (black bars) fed a high-fat diet for 4 weeks was significantly decreased at 11 and 20 mmol/l glucose vs wild-type mice (white bars) (n=4). (**b**) Insulin secretion of *Hipk3*$^{\square/\square}$ and wild-type islets in the presence of KCl and glibenclamide. (**c**) Islets from *Hipk3*$^{\square/\square}$ (continuous line) and wild-type (dashed line) mice were perifused with a medium containing 20 mmol/l glucose and 20 mmol/l KCl (n=4). (**d**) Changes in ATP content in islets from wild-type and *Hipk3*$^{\square/\square}$ mice after glucose stimulation for 1 h (n=4). (**e**) The increase in calcium concentration in response to glucose was impaired in *Hipk3*$^{-/-}$ islets (n=6). Glucose-stimulated Ca^{2+} influx in single beta cells was measured with the Ca^{2+} indicator fura-2. Fura-2 post-stimulation fluorescence (F) was normalised to resting fluorescence ($F0$). (**f**) Changes in beta cell mass during consumption of a high-fat (HF) diet. The insulin content of islets was decreased in *Hipk3*$^{\square/\square}$ vs wild-type mice at week 12 of an HF diet. (**g**) Insulin content per pancreas was compared between *Hipk3*$^{\square/\square}$ and wild-type mice (n=4). Data represent means±SEM; *p<0.05 and **p<0.01 compared with wild-type control mice

fat diet (Fig. 4f, g). Similarly, the proportion of islets to total area of dissected pancreas from *Hipk3*$^{\square/\square}$ mice was not decreased at week 4 of a high-fat diet, but was significantly decreased at week12 of a high-fat diet (Fig. 5a, b). We estimated beta cell proliferation on the basis of PCNA staining. During high-fat diet conditions, significantly more PCNA-positive cells were observed in the islets of wild-type mice than in *Hipk3*$^{\square/\square}$ mice (Fig. 5a, c). We estimated islet cell apoptosis on the basis of TUNEL staining. During high-fat diet conditions, significantly more TUNEL-positive cells were observed in the islets of wild-type mice than in *Hipk3*$^{\square/\square}$ mice (Fig. 5a, d). In summary, HIPK3 has an effect on beta cell secretory function, beta cell proliferation and apoptosis.

Decreased PDX1 and GSK3β phosphorylation in the absence of Hipk3 To identify the mechanism underlying the loss of glucose-stimulated insulin secretion and beta cell proliferation, we evaluated the mediators of HIPK3-regulated genes relative to islet function. Expression of *Pdx1*, a beta cell-specific transcription factor, was significantly decreased in the islets of *Hipk3*$^{-/-}$ mice fed a high-fat diet for 12 weeks, falling by approximately 50% (Fig. 6a, m, n). Notably, we detected decreases of 34% and 30% in *Gck* and *Slc2a2* mRNA expression in *Hipk3*$^{\square/\square}$ mice, indicating that loss of HIPK3 negatively modulates the expression of these genes that encode glucose-sensing proteins (Fig. 6b, c). Moreover, we observed significantly reduced mRNA levels of *Hnf4a* and *Tcf7l2* in *Hipk3*$^{\square/\square}$

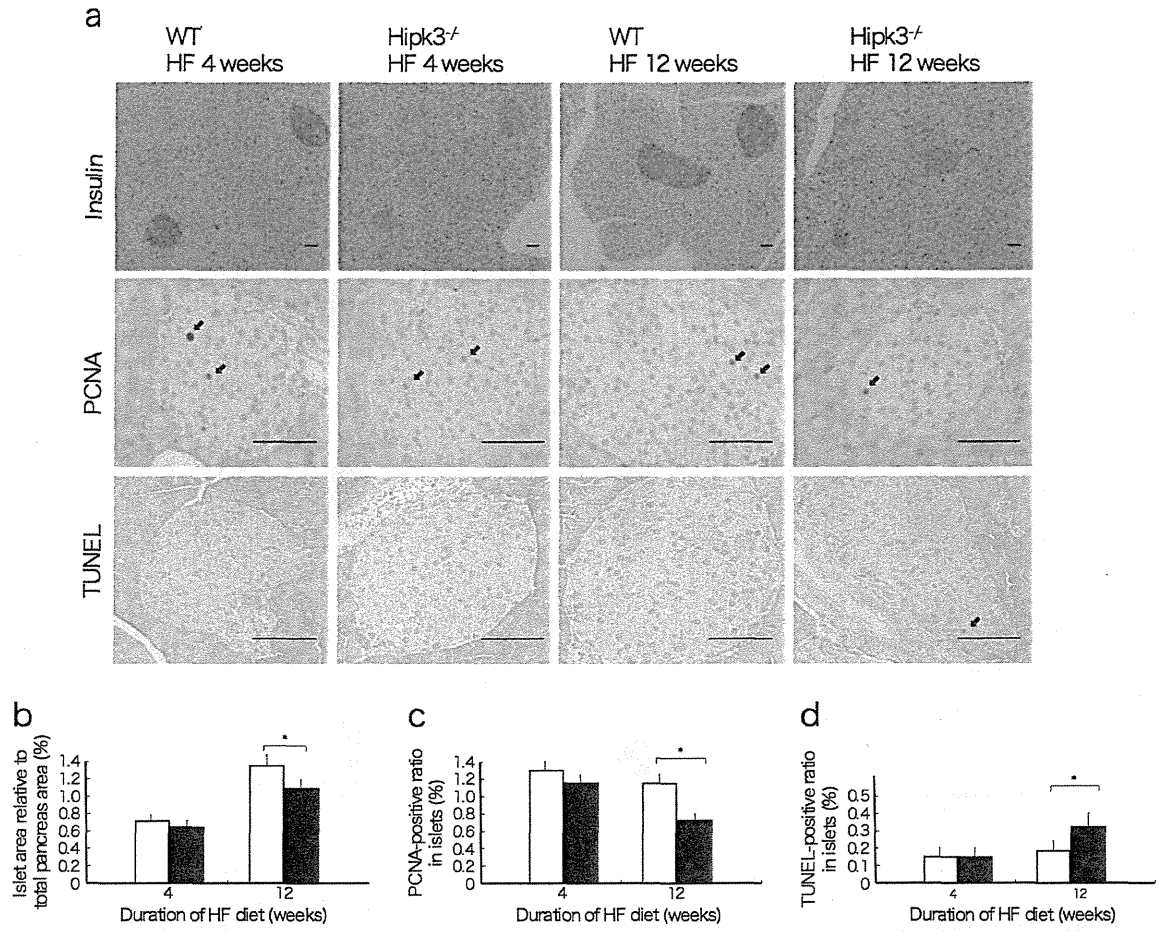

Fig. 5 (**a**) PCNA immune staining analysis was based on the counting of 1,662 and 1,879 cells, respectively, per islet sample from wild-type (WT) (n=4) and *Hipk3*$^{\square/\square}$ (n=4) mice fed a high-fat diet for 4 weeks, and (high-fat diet, 12 weeks) on the counting of 1,674 and 1,518 cells, respectively, per islet sample from wild-type (n=4) and *Hipk3*$^{\square/\square}$ (n=4) mice. Tissues were processed for paraffin embedding, and 4 μm sections were cut and mounted on silanised slides. Pancreatic sections were stained with anti-insulin and anti-PCNA antibodies as indicated. We estimated islet cell apoptosis on the basis of TUNEL staining. Scale bars, 100 μm. (**b**) The proportion of islet to total area was decreased in *Hipk3*$^{\square/\square}$ compared with wild-type mice fed a HF diet (n=4). (**c**) Replication rate of beta cells from *Hipk3*$^{\square/\square}$ and wild-type mice (n=4). (**d**) The apoptosis rate of islet cells from *Hipk3*$^{\square/\square}$ and wild-type mice (n=4). Data represent means±SEM; *p<0.05 compared with wild-type control mice

islets, suggesting that HIPK3 plays a role in influencing the expression of transcription factors. Additionally, cyclin D1 gene expression (Fig. 6d), GSK3β phosphorylation (Fig. 6m, o) and β-catenin abundance (Fig. 6m, p) were decreased in the islets of *Hipk3*$^{-/-}$ mice, indicating a role of HIPK3 in Wnt signalling. Histological analysis showed that nuclear PDX1 abundance was significantly decreased in the islets of *Hipk3*$^{-/-}$ mice fed a high-fat diet for 12 weeks (Fig. 6q, r). Histological analysis also showed that GSK3β phosphorylation was decreased in the islets of *Hipk3*$^{-/-}$ mice (Fig. 6s).

Wnt signalling lessens the decrease in insulin secretion induced by loss of Hipk3 We investigated whether Wnt signalling can also increase glucose-stimulated insulin secretion in *Hipk3*$^{-/-}$ islets. Wnt3a enhanced insulin secretion by 19% in *Hipk3*$^{-/-}$ islets (Fig. 7a) upon 20 mmol/l glucose stimulation. We also found that the GSK3 inhibitor LiCl and 1-azakenpaullone treatment enhanced insulin secretion in *Hipk3*$^{-/-}$ islets by 31% and 28%, respectively, upon 20 mmol/l glucose stimulation (Fig. 7b, c). These observations suggest that impaired Wnt signalling caused by *Hipk3* deficiency leads to impaired beta cell function.

Discussion

It is becoming increasingly clear that the diverse biological consequences of the loss of HIPK activity include the coordinated death of cells in earlier developmental stages and the dysregulation of proper cell number in diverse tissue types. Mice that are deficient for *Hipk1* and *Hipk2* singly have a normal overall appearance, a finding that is probably due to a functional redundancy between HIPK1 and HIPK2 [41]. However, *Hipk1*$^{\square/\square}$; *Hipk2*$^{\square/\square}$ mice are progressively lost in

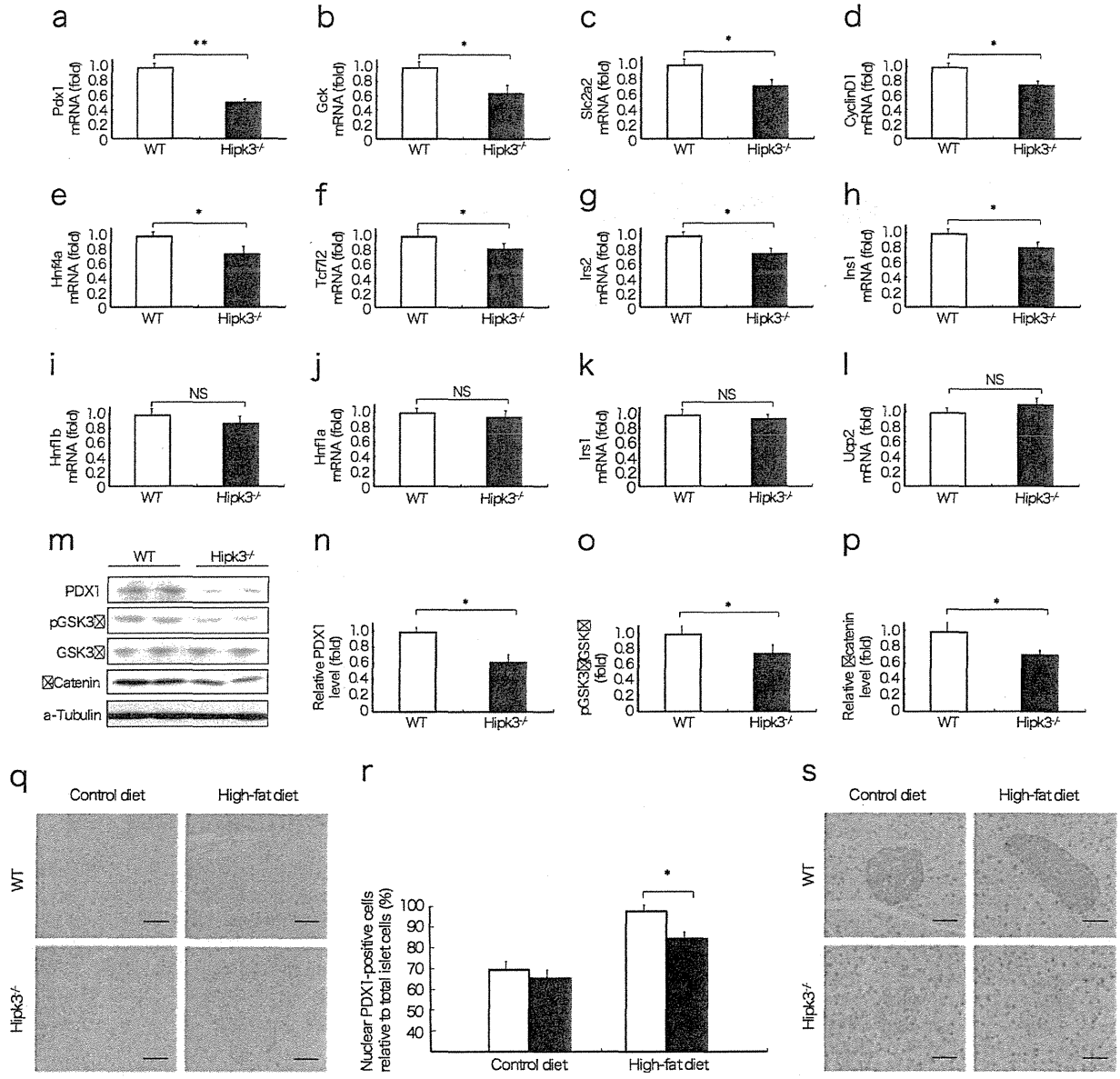

Fig. 6 (**a**) Quantitative RT-PCR analysis of islet-enriched transcription factors and glucose-sensing proteins *Pdx1*, (**b**) *Gck*, (**c**) *Slc2a2*, (**d**) Cyclin D1, (**e**) *Hnf4a*, (**f**) *Tcf7l2*, (**g**) *Irs2*, (**h**) *Ins1*, (**i**) *Hnf1b*, (**j**) *Hnf1a*, (**k**) *Irs1* and (**l**) *Ucp2*. Analysis was in islets isolated from wild-type (WT) and *Hipk3*$^{\square/\square}$ mice (n=4) on a high-fat diet for 12 weeks. Samples were normalised to *Gapdh*. **m** Protein samples from lysates of isolated islets from *Hipk3*$^{\square/\square}$ mice were separated by SDS-PAGE and western blot analyses performed using the antibodies as labelled (n=4). (**n**) Quantification of relative PDX1, (**o**) pGSK3β and (**p**) β-catenin levels. (**q**) Pancreatic sections were stained with anti-PDX1 antibody. PDX1 immune staining analysis was based on the counting of 1,845 and 1,683 cells, respectively, per islet sample from wild-type (n=4) and *Hipk3*$^{\square/\square}$ (n=4) mice fed a high-fat diet for 12 weeks, and (control diet) on the counting of 1,545 and 1,609 cells, respectively, per islet sample from wild-type (n=4) and *Hipk3*$^{\square/\square}$ (n=4) mice. (**r**) Ratio of the number of nuclear PDX1-positive cells to the total number of islet cells. (**s**) Histological analysis of pancreatic islet phosphorylated GSK3β in wild-type and *Hipk3*$^{\square/\square}$ mice. Pancreatic sections were stained with anti-phspho-GSK3β(Ser9) antibodies. Analysis was based on the counting of 1,705 and 1,692 cells, respectively, per islet sample from wild-type (n=4) and *Hipk3*$^{\square/\square}$ (n=4) mice fed a high-fat diet for 12 weeks, and (control diet) on the counting of 1,875 and 1,586 cells, respectively, per islet sample from wild-type (n=4) and *Hipk3*$^{\square/\square}$ (n=4) mice. Scale bars (**q**, **s**), 100 μm. Data represent means±SEM; *p<0.05 and **p<0.01 compared with wild-type control mice

utero, and exhibit exencephaly and severe defects in haematopoiesis, vasculogenesis and angiogenesis. In our experiments, expression of Hipk genes was detected in adult islets, and the HIPK family additively regulated insulin secretion. Our data also indicate that high-fat diet leads most significantly to *Hipk3* upregulation. The other two Hipk genes correlate with glucose tolerance and may play roles in glucose homeostasis. Given the inability of the intact *Hipk3* gene to support early development in *Hipk1*$^{\square/\square}$; *Hipk2*$^{\square/\square}$ mice and the contribution of HIPK3 to impaired

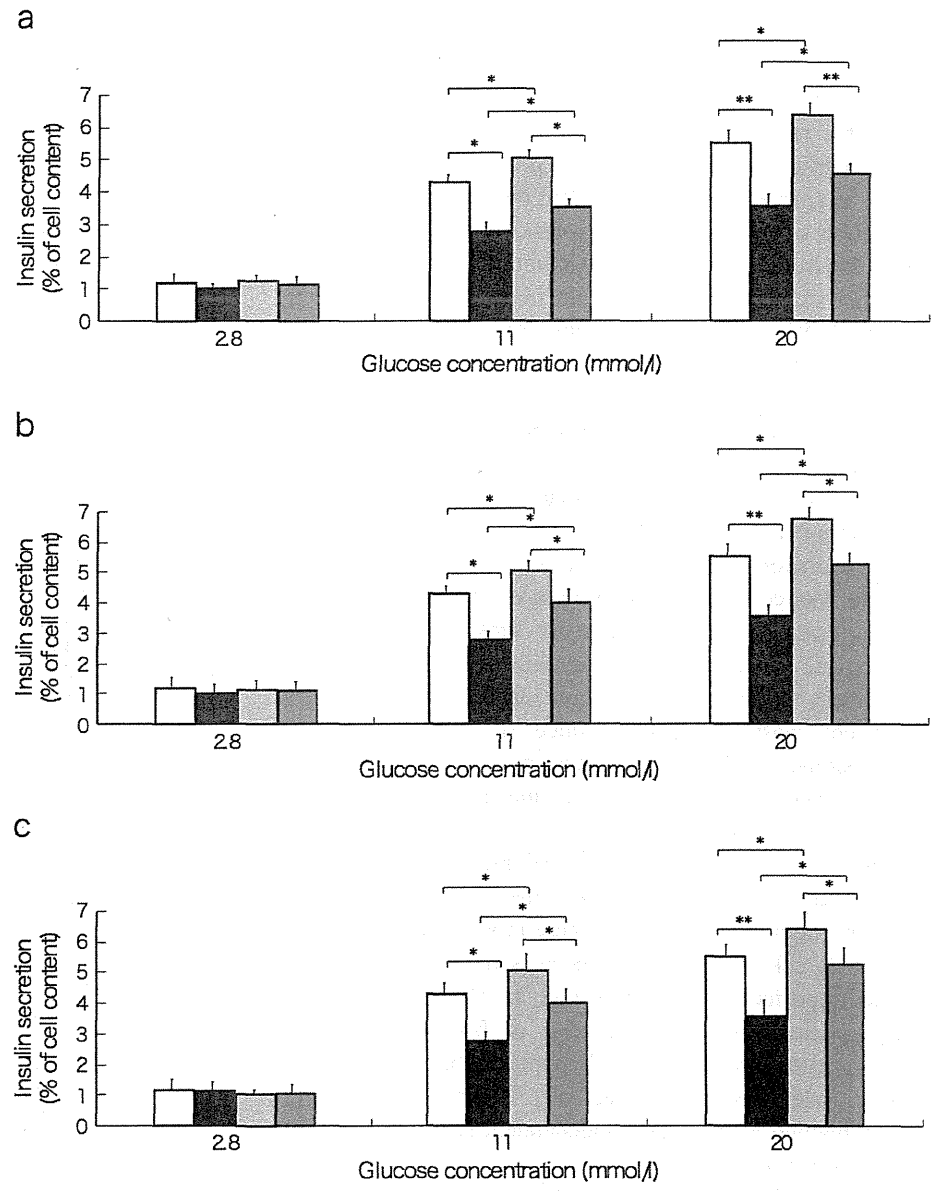

Fig. 7 Wnt3a regulates HIPK3-induced insulin secretion. (**a**) Insulin secretion was decreased by Wnt3a (n=4). Insulin secretion by islets from wild-type (white bars; light grey bars, wild-type+Wnt3a) and *Hipk3*$^{\square/\square}$ (black bars; dark grey bars, *Hipk3*$^{\square/\square}$+Wnt3a) mice was measured in KRB with a glucose concentration of 2.8, 11 or 20 mmol/l. Static incubation was performed for 1 h on ten islets per tube at 37°C, after preincubation with the basal glucose concentration for 20 min. Insulin levels were determined with a mouse insulin ELISA kit. (**b**) The insulin secretion of isolated islets was decreased by *Hipk3* deficiency and increased by the GSK3 inhibitor LiCl (n=4). Key, as above (**a**), except: light grey bars, wild-type+LiCl; dark grey bars, *Hipk3*$^{\square/\square}$+LiCl. (**c**) Insulin secretion of isolated islets from *Hipk3*$^{\square/\square}$ mice was increased by Wnt signalling activation by the GSK3 inhibitor, 1-azakenpaullone (n=4). Key, as above (**a**), except: light grey bars, wild-type+1-azakenpaullone; dark grey bars, *Hipk3*$^{\square/\square}$+1-azakenpaullone. Data represent means±SEM; *p<0.05 and **p<0.01

insulin secretion, we anticipate that HIPK3 may serve unique physiological roles especially in diabetes-prone circumstances such as a high-fat diet.

We also analysed *Hipk3*$^{-/-}$ mice. Major changes in gene phenotype were found with very modest increases in glucose levels, such as impaired glucose tolerance. Changes in islet gene expression can be explained by *Hipk3* deficiency and glucose toxicity.

HIPK2 positively influences PDX1 levels and transcriptional activity, and directly phosphorylates the C-terminal portion of PDX1 [28]. HIPK2 is a potential kinase for PDX1 Ser-269, with high glucose concentrations decreasing the degree of phosphorylation on PDX1 Ser-269 in beta cells [42]. We showed that the number of PDX1-positive cells was reduced by 20% in *Hipk3*-knockout mice on a 12 week high-fat diet (Fig. 6r). The insulin content was reduced by 18% in the same conditions (Fig. 4f). Thus, we speculate that decreased PDX1 positivity is related to beta cell mass reduction. Considering the role of PDX1 in beta cells and non-beta cells, HIPK may affect beta cells and non-beta cells, and reduce beta cell mass. Further studies are needed to clarify the mechanisms of beta cell reduction that decreased PDX1 positivity. HIPK3 has been shown to augment transcription of androgen receptor [32], SF-1 [35] and runt-related transcription factor 2 [36]. In this study, we identified HIPK3 as a novel modulator of PDX1 abundance. Several transcription factors converge on regulatory areas within the *Pdx1* promoter [43–45], including NKx2.2, a member of the NK-2 family of homeobox genes [44, 45]. HIPKs possess a homeodomain-interacting domain that is important for enhancing the repressor activities of NK homeodomain transcription factors [22], allowing the

possibility that HIPK3 may affect PDX1 levels via interacting factors that promote PDX1 transcription.

We showed that insulin transcript levels are correlated with the results of luciferase assays. We used rat insulin promoter instead of mouse insulin promoter, and this difference in species may have affected our results. Concerning the effect of HIPK on insulin expression, HIPK may interact with the insulin promoter or act by modulating PDX1 levels. Further studies are needed to elucidate the mechanisms by which HIPK affects insulin expression.

This study also revealed the involvement of the Wnt–GSK3β–β-catenin cascade in the action of HIPK3. Wnt signalling influences endocrine pancreas development and modulates mature beta cell functions, including insulin secretion, beta cell survival and beta cell proliferation [6–9]. Treatment with Wnt ligands increases glucose-induced insulin secretion in wild-type islets, but not in islets deficient in the Wnt co-receptor, lipoprotein receptor-related protein 5, suggesting a deficit in glucose sensing in islets when canonical Wnt signalling is impaired [46]. β-Catenin is sufficient to induce proliferation markers and to increase beta cell mass in transgenic mice [4]. Adipocyte-derived Wnt signalling molecules induce cyclin D1 transcription, and the proliferation of beta cell lines and primary murine beta cells [5]. Beta cell-specific *Gsk3b* knockout prevents diabetes in *Irs2*-knockout [13] and high-fat diet-fed mice [14] through expanded beta cell mass with increased beta cell proliferation. In line with these reports, we have shown that beta cell proliferation is decreased in *Hipk3*$^{\square/\square}$ mouse islets upon feeding a high-fat diet. In contrast to our findings, pancreas-specific depletion of β-catenin has been shown to lead to acinar cell hypoplasia, but not to change the mass and function of islets [47]. This discrepancy might be explained by β-catenin-independent signal transduction downstream of HIPK3.

Previous reports indicate that β-catenin and transcription factor 7 like 2, T cell specific, HMG box regulate proglucagon gene expression and GLP-1 synthesis in enteroendocrine cells [48, 49]. In this study, we obtained evidence that HIPK3 deficiency lowered GLP-1 concentrations and impaired glucose tolerance. It can thus be speculated that HIPK3 activates the Wnt signalling pathway for GLP-1 synthesis and secretion. Furthermore, HIPK3 may alter the response of intestinal K cells to known secretagogues, including nutrients, fatty acids and related molecules. These hypotheses deserve further examination.

In conclusion, HIPK3 has a role in insulin secretion, affecting the levels of pancreatic PDX1 and GSK3β phosphorylation. Thus, targeting HIPK3 with novel agonists could lead to new therapeutic strategies for preserving beta cell function. The present results provide new insight into the pathogenesis of type 2 diabetes.

Acknowledgements We thank M. Yamaguchi and N. Miyama (Department of Diabetes and Metabolic Disease, University of Tokyo, Tokyo, Japan) for their excellent technical assistance.

Funding This work was supported by a grant for Translational Systems Biology and Medicine Initiative (TSBMI) from the Ministry of Education, Culture, Sports, Science and Technology of Japan (to T. Kadowaki), a Grant-in-aid for Scientific Research in Priority Areas (S) from the Ministry of Education, Culture, Sports, Science and Technology of Japan (to T. Kadowaki), Health Science Research grants (Research on Human Genome and Gene Therapy) from the Ministry of Health and Welfare (to T. Kadowaki) and a Grant-in-Aid from the Japan Society for the Promotion of Science (JSPS) (to T. Kadowaki and K. Hara).

Duality of interest The authors declare that there is no duality of interest associated with this manuscript.

Contribution statement NS, KH and TK planned and designed the study. NS, KH, KU and TK conceived and designed the experiments, and wrote the manuscript. HF and MH contributed to the conception and design, the analysis and interpretation of the data, and drafting the article. NT carried out the two-photon excitation imaging and contributed to drafting the article. IT, MO, HA, MN, NK and TY provided advice, and contributed to the conception and interpretation of the data and drafting the article. All authors approved the final version.

References

1. Kahn CR (1994) Banting lecture. Insulin action, diabetogenes, and the cause of type II diabetes. Diabetes 43:1066–1084
2. Accili D (2004) Lilly lecture 2003: the struggle for mastery in insulin action: from triumvirate to republic. Diabetes 53:1633–1642
3. Doria A, Patti ME, Kahn CR (2008) The emerging genetic architecture of type 2 diabetes. Cell Metab 8:186–200
4. Rulifson IC, Karnik SK, Heiser PW et al (2007) Wnt signaling regulates pancreatic beta cell proliferation. Proc Nat Acad Sci USA 104:6247–6252
5. Schinner S, Ulgen F, Papewalis C et al (2008) Regulation of insulin secretion, glucokinase gene transcription and beta cell proliferation by adipocyte-derived Wnt signalling molecules. Diabetologia 51:147–154
6. Liu Z, Habener JF (2010) Wnt signaling in pancreatic islets. Adv Exp Med Biol 654:391–419
7. Welters HJ, Kulkarni RN (2008) Wnt signaling: relevance to beta-cell biology and diabetes. Trends Endocrinol Metab 19:349–355
8. Jin T (2008) The WNT signalling pathway and diabetes mellitus. Diabetologia 51:1771–1780
9. Schinner S, Willenberg HS, Schott M, Scherbaum WA (2009) Pathophysiological aspects of Wnt-signaling in endocrine disease. Eur J Endocrinol 160:731–737
10. Logan CY, Nusse R (2004) The Wnt signaling pathway in development and disease. Annu Rev Cell Dev Biol 20:781–810
11. Moon RT, Kohn AD, de Ferrari GV, Kaykas A (2004) WNT and beta-catenin signalling: diseases and therapies. Nat Rev Genet 5:691–701
12. Liu Z, Tanabe K, Bernal-Mizrachi E, Permutt MA (2008) Mice with beta cell overexpression of glycogen synthase kinase-3beta have reduced beta cell mass and proliferation. Diabetologia 51:623–631

13. Tanabe K, Liu Z, Patel S et al (2009) Genetic deficiency of glycogen synthase kinase-3beta corrects diabetes in mouse models of insulin resistance. PLoS Biol 6:e37
14. Liu Y, Tanabe K, Baronnier D et al (2010) Conditional ablation of Gsk-3β in islet beta cells results in expanded mass and resistance to fat feeding-induced diabetes in mice. Diabetologia 53:2600–2610
15. Kanei-Ishii C, Ninomiya-Tsuji J, Tanikawa J et al (2004) Wnt-1 signal induces phosphorylation and degradation of c-Myb protein via TAK1, HIPK2, and NLK. Genes Dev 18:816–829
16. Wei G, Ku S, Ma G et al (2007) HIPK2 represses beta-catenin-mediated transcription, epidermal stem cell expansion, and skin tumorigenesis. Proc Natl Acad Sci USA 104:13040–13045
17. Kim EA, Kim JE, Sung KS et al (2010) Homeodomain-interacting protein kinase 2 (HIPK2) targets beta-catenin for phosphorylation and proteasomal degradation. Biochem Biophys Res Commun 394:966–971
18. Swarup S, Verheyen EM (2011) Drosophila homeodomain-interacting protein kinase inhibits the Skp1-Cul1-F-box E3 ligase complex to dually promote Wingless and Hedgehog signaling. Proc Natl Acad Sci USA 108:9887–9892
19. Lee W, Swarup S, Chen J, Ishitani T, Verheyen EM (2009) Homeodomain-interacting protein kinases (Hipks) promote Wnt/Wg signaling through stabilization of beta-catenin/Arm and stimulation of target gene expression. Development 136:241–251
20. Louie SH, Yang XY, Conrad WH et al (2009) Modulation of the beta-catenin signaling pathway by the dishevelled-associated protein Hipk1. PLoS One 4:e4310
21. Hisaka H, Ezan J, Itoh K, Li X, Klymkowsky MW, Sokol SY (2010) Regulation of TCF3 by Wnt-dependent phosphorylation during vertebrate axis specification. Dev Cell 19:521–532
22. Kim YH, Choi CY, Lee SJ, Conti MA, Kim Y (1998) Homeodomain-interacting protein kinases, a novel family of co-repressors for homeodomain transcription factors. J Biol Chem 273:25875–25879
23. D'Orazi G, Cecchinelli B, Bruno T et al (2002) Homeodomain-interacting protein kinase-2 phosphorylates p53 at Ser 46 and mediates apoptosis. Cell Biol 4:11–19
24. Hofmann TG, Moller A, Sirma H et al (2002) Regulation of p53 activity by its interaction with homeodomain-interacting protein kinase-2. Nat Cell Biol 4:1–10
25. Kondo S, Lu Y, Debbas M et al (2003) Characterization of cells and gene-targeted mice deficient for the p53-binding kinase homeodomain-interacting protein kinase 1 (HIPK1). Proc Natl Acad Sci USA 100:5431–5436
26. Zhang Q, Yoshimatsu Y, Hildebrand J, Frisch SM, Goodman RH (2003) Homeodomain interacting protein kinase 2 promotes apoptosis by downregulating the transcriptional corepressor CtBP. Cell 115:177–186
27. Choi CY, Kim YH, Kim YO et al (2005) Phosphorylation by the DHIPK2 protein kinase modulates the corepressor activity of Groucho. J Biol Chem 280:21427–21436
28. Boucher M, Simoneau ML, Edlund H (2009) The homeodomain-interacting protein kinase 2 regulates insulin promoter factor-1/pancreatic duodenal homeobox-1 transcriptional activity. Endocrinology 150:87–97
29. Jonsson J, Carlsson L, Edlund T, Edlund H (1994) Insulin-promoter-factor 1 is required for pancreas development in mice. Nature 371:606–609
30. Offield MF, Jetton TL, Labosky PA et al (1996) PDX-1 is required for pancreatic outgrowth and differentiation of the rostral duodenum. Development 122:983–995
31. Stoffers DA, Zinkin NT, Stanojevic V, Clarke WL, Habener JF (1997) Pancreatic agenesis attributable to a single nucleotide deletion in the human IPF1 gene coding sequence. Nat Genet 15:106–110
32. Moilanen AM, Karvonen U, Poukka H, Janne OA, Palvimo JJ (1998) Activation of androgen receptor function by a novel nuclear protein kinase. Mol Biol Cell 9:2527–2543
33. Rochat-Steiner V, Becker K, Micheau O, Schneider P, Burns K, Tschopp J (2000) FIST/HIPK3: a Fas/FADD-interacting serine/threonine kinase that induces FADD phosphorylation and inhibits fas-mediated Jun NH(2)-terminal kinase activation. J Exp Med 192:1165–1174
34. Curtin JF, Cotter TG (2004) JNK regulates HIPK3 expression and promotes resistance to Fas-mediated apoptosis in DU 145 prostate carcinoma cells. J Biol Chem 279:17090–17100
35. Lan HC, Li HJ, Lin G, Lai PY, Chung BC (2007) Cyclic AMP stimulates SF-1-dependent CYP11A1 expression through homeodomain-interacting protein kinase 3-mediated Jun N-terminal kinase and c-Jun phosphorylation. Mol Cell Biol 27:2027–2036
36. Sierra OL, Towler DA (2010) Runx2 trans-activation mediated by the MSX2-interacting nuclear target requires homeodomain interacting protein kinase-3. Mol Endocrinol 24:1478–1497
37. Inoue T, Kagawa T, Inoue-Mochita M et al (2010) Involvement of the Hipk family in regulation of eyeball size, lens formation and retinal morphogenesis. FEBS Lett 584:3233–3238
38. Scopsi L, Wang BL, Larsson LI (1986) Nonspecific immunocytochemical reactions with certain neurohormonal peptides and basic peptide Sequences. J Histochem Cytochem 34:1469–1475
39. Noda M, Yamashita S, Takahashi N et al (2002) Switch to anaerobic glucose metabolism with NADH accumulation in the beta-cell model of mitochondrial diabetes. Characteristics of betaHC9 cells deficient in mitochondrial DNA transcription. J Biol Chem 277:41817–41826
40. Takahashi N, Hatakeyama H, Okado H et al (2004) Sequential exocytosis of insulin granules is associated with redistribution of SNAP25. J Cell Biol 165:255–262
41. Isono K, Nemoto K, Li Y et al (2006) Overlapping roles for homeodomain-interacting protein kinases hipk1 and hipk2 in the mediation of cell growth in response to morphogenetic and genotoxic signals. Mol Cell Biol 26:2758–2771
42. An R, da Silva Xavier G, Semplici F et al (2010) Pancreatic and duodenal homeobox 1 (PDX1) phosphorylation at serine-269 is HIPK2-dependent and affects PDX1 subnuclear localization. Biochem Biophys Res Commun 399:155–161
43. Gerrish K, Gannon M, Shih D et al (2000) Pancreatic beta cell-specific transcription of the pdx-1 gene. The role of conserved upstream control regions and their hepatic nuclear factor 3beta sites. J Biol Chem 275:3485–3492
44. Gerrish K, van Velkinburgh JC, Stein R (2004) Conserved transcriptional regulatory domains of the pdx-1 gene. Mol Endocrinol 18:533–548
45. van Velkinburgh JC, Samaras SE, Gerrish K, Artner I, Stein R (2005) Interactions between areas I and II direct pdx-1 expression specifically to islet cell types of the mature and developing pancreas. J Biol Chem 280:38438–38444
46. Fujino T, Asaba H, Kang MJ et al (2003) Low-density lipoprotein receptor-related protein 5 (LRP5) is essential for normal cholesterol metabolism and glucose-induced insulin secretion. Proc Natl Acad Sci USA 100:229–234
47. Murtaugh LC, Law AC, Dor Y, Melton DA (2005) Beta-catenin is essential for pancreatic acinar but not islet development. Development 132:4663–4674
48. Yi F, Brubaker PL, Jin T (2005) TCF-4 mediates cell type-specific regulation of proglucagon gene expression by beta-catenin and glycogen synthase kinase-3beta. J Biol Chem 280:1457–1464
49. Ni Z, Anini Y, Fang X, Mills G, Brubaker PL, Jin T (2003) Transcriptional activation of the proglucagon gene by lithium and beta-catenin in intestinal endocrine L cells. J Biol Chem 278:1380–1387

Rev Endocr Metab Disord (2013) 14:207–216
DOI 10.1007/s11154-013-9242-z

The role of endothelial insulin signaling in the regulation of glucose metabolism

Tetsuya Kubota · Naoto Kubota · Takashi Kadowaki

Published online: 16 April 2013

Abstract The skeletal muscle is one of the major target organs of insulin and plays an essential role in insulin-induced glucose uptake. Some evidence indicates that insulin delivery to skeletal muscle interstitium through the endothelial cells is the rate-limiting step in insulin-stimulated glucose uptake. Researchers have also found that this process is impaired by insulin resistance in type 2 diabetes and obesity. A recent study of ours demonstrated that insulin signaling in the endothelial cells plays a pivotal role in the regulation of glucose uptake by the skeletal muscle. Specifically, impaired insulin signaling in the endothelial cells, with reduction of insulin-induced eNOS phosphorylation, causes attenuation of the insulin-induced capillary recruitment and insulin delivery, which, in turn reduces glucose uptake by the skeletal muscle in high-fat diet-fed mice. Moreover, restoration of the insulin-induced eNOS phosphorylation in the endothelial cells completely reverses the reduction in the capillary recruitment and insulin delivery, and as a result, significantly restores glucose uptake by the skeletal muscle. In the present review, we describe the recent progress in research on the physiological and pathophysiological roles of endothelial insulin signaling in the regulation of insulin-induced glucose uptake by the skeletal muscle.

Keywords Insulin signaling · Endothelial cell · Capillary recruitment · Skeletal muscle insulin resistance · Endothelial nitric oxide synthase · Insulin transport

1 Introduction

In recent years there has been a rapid growth in the incidence of type 2 diabetes in both Western and Asian countries [1, 2]. The increasing incidence of type 2 diabetes is most likely due to genetic factors and pathological processes among the ageing population exposed to negative health effects of certain lifestyle, including diets high in fat combined with reduced levels of exercise [1]. Type 2 diabetes magnifies the risk of cardiovascular mortality, which is corollary to a growing epidemic of micro- and macro-vascular complications, including diabetic nephropathy and coronary artery disease [3, 4]. Moreover, high prevalence of type 2 diabetes is associated with a significant economic burden [5]. It is important to elucidate the precise molecular mechanisms underlying the development and progression of type 2 diabetes.

Skeletal muscle plays an essential role in the maintenance of normal blood glucose concentrations and is one of the major sites of insulin resistance in type 2 diabetic patients [6]. Excess lipid storage in adipose tissue leads to accumulation of intracellular lipid derivatives (diacylglycerol and ceramides), inflammation and oxidative stress in the skeletal muscle. As a result, intramyocellular insulin signaling is impaired, thereby causing skeletal muscle insulin resistance [7–10]. The impairment of insulin intracellular signaling pathways within the myocytes caused by ectopic fat accumulation is considered to be a major mechanism underlying skeletal muscle insulin resistance (Fig. 1a). These researches are comprehensively reviewed elsewhere [11, 12].

On the other hand, in order to stimulate insulin-induced glucose uptake by the skeletal muscle, insulin has to be

Tetsuya Kubota and Naoto Kubota contributed equally to this work.

T. Kubota · N. Kubota (✉) · T. Kadowaki (✉)
Department of Diabetes and Metabolic Diseases, Graduate School of Medicine, University of Tokyo, 7-3-1 Hongo, Bunkyo-ku, Tokyo 113-8655, Japan
e-mail: nkubota-tky@umin.ac.jp
e-mail: kadowaki-3im@h.u-tokyo.ac.jp

T. Kubota · N. Kubota
Clinical Nutrition Program, National Institute of Health and Nutrition, Tokyo 162-8636, Japan

N. Kubota · T. Kadowaki
Translational Systems Biology and Medicine Initiative (TSBMI), University of Tokyo, Tokyo 153-8515, Japan

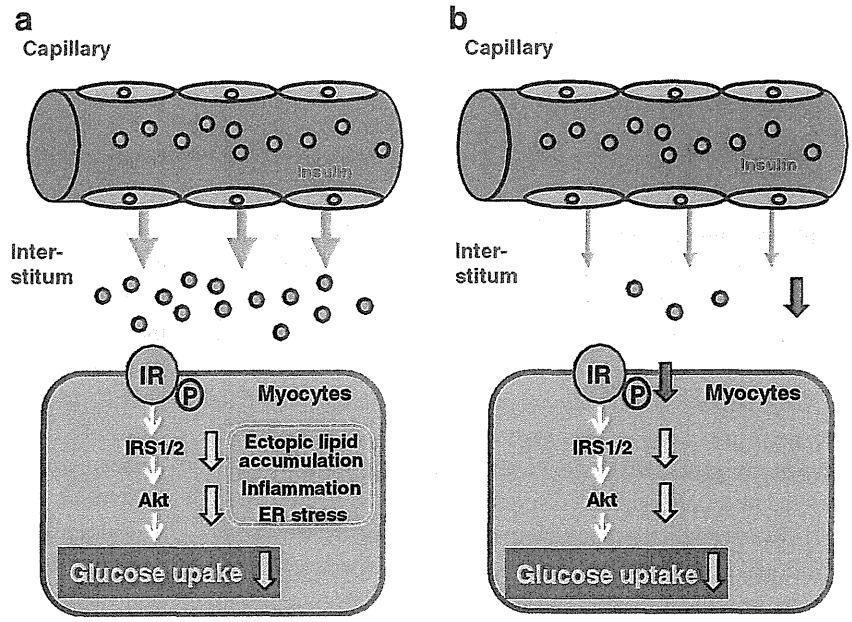

Fig. 1 Two models of skeletal muscle insulin resistance. a Impairment of cellular signaling within the myocytes. b Impairment of insulin delivery to skeletal muscle

delivered into the capillaries and cross the endothelial barrier to enter the interstitial spaces [13]. Some evidence indicates that insulin delivery to skeletal muscle interstitium through the endothelial cells is the rate-limiting step in insulin-stimulated glucose uptake by the skeletal muscle and that this process is impaired in insulin resistance with type 2 diabetes and obesity [14–16]. In addition to an impairment of cellular signaling within the myocytes, there is an impairment of insulin delivery to skeletal muscle as a major mechanism underlying skeletal muscle insulin resistance (Fig. 1b).

In this review, we describe recent progress in research on the physiological and pathophysiological roles of endothelial insulin signaling in the regulation of insulin-induced glucose uptake by the skeletal muscle.

2 Insulin action in the endothelial cells

There are two major pathways in insulin signaling of endothelial cells: phosphoinositide 3 (PI3) kinase-Akt and RAS-mitogen activated protein (MAP) kinase pathway [17, 18].

Insulin action is initiated by the binding of the insulin molecule to its specific cell surface receptor [19]. Insulin binding to its receptor results in the tyrosine phosphorylation of the insulin receptor substrate (IRS) by the insulin receptor tyrosine kinase. Although the IRS family is represented by IRS-1, 2, 3, 4, 5 and 6 [20], IRS-1 and 2 are particularly important in endothelial cells [21, 22]. Phosphorylated IRSs allow association of IRSs with the regulatory subunit of PI3 kinase. PI3 kinase activates 3-phosphoinositide-dependent protein kinase 1 (PDK1), which activates Akt, a serine kinase. Akt directly phosphorylates eNOS at Ser1177, resulting in increased eNOS activity and nitric oxide (NO) production [23–25]. NO mediates vasodilation mainly by diffusion to vascular smooth muscle cells, where it activates soluble guanylate cyclase, resulting in the formation of cyclic guanosine monophosphate (cGMP) [26, 27].

In addition to eNOS activation, insulin signaling in the endothelial cells regulates vasoconstrictor endothelin (ET)-1 expression [28, 29]. Insulin activates IR and allows binding of the intracellular mediator Shc to the Src homology 2 domain of growth factor receptor-bound protein 2 (Grb2). This, in turn, leads to activation of the Son of Sevenless (SOS) and Ras, which then initiates a kinase phosphorylation cascade involving Raf, MAP kinase kinase pathway [30]. Activation of the MAP kinase induces the secretion of ET-1. The secreted ET-1 binds to its receptor, ET-1_A and ET-1_B, and activates PKC in vascular smooth muscle cells. PKC activation by ET-1 leads to contraction in the vascular smooth muscle cells [31]. A MAP kinase inhibitor completely suppressed insulin-stimulated ET-1 expression, although pretreatment with wortmannin, a PI3 kinase inhibitor, did not significantly affect insulin-stimulated ET-1 expression [32].

Two major pathways of insulin signaling in endothelial cells regulate distinct biological functions. A critical balance between endothelium-derived relaxing and contracting factors maintains vascular homeostasis.

3 Selective insulin resistance of endothelial cells in obese models

Interestingly, PI3 kinase-Akt pathway alone is impaired in the endothelial cells of obese and type 2 diabetes models [33, 34]. King and colleagues found the activity of IRS-2

associated PI3 kinase was impaired in the vasculature of obese Zucker rats [35]. On the other hand, the MAP kinase pathway remains unchanged in the vasculature [36]. Jansson and colleagues reported that in microvascular endothelial cells isolated from type 2 diabetes subjects, the phosphorylation of Akt in response to insulin attenuated, whereas insulin-stimulated phosphorylation of extracellular signal-related kinase (ERK)1/2 was increased [37]. In reference to these phenomena, King has coined the phrase 'selective insulin resistance' of endothelial cells in obese models [27].

Why is only the PI3 kinase pathway of endothelial cells impaired in obesity? IRS-2 expression levels dropped markedly in the endothelial cells of both ob/ob and high-fat (HF) diet-fed mice, although ET-1 expression remained unchanged [38]. To elucidate the mechanisms by which the expression of IRS-2 was downregulated, we conducted an experiment using human umbilical arterial endothelial cells (HUAEC). The expression of IRS-2 was significantly suppressed from 3 h onwards after insulin treatment. The promoter region of the IRS-2 gene contains an insulin response element, which is recognised by forkhead transcription factor O1 (FoxO1) [39, 40]. To investigate the relationship between IRS-2 and FoxO1, endothelial cells were immunostained with FoxO1 antibody after insulin treatment. The expression of IRS-2 was significantly suppressed in parallel with FoxO1 translocation from the nuclei to the cytosol, and the expression was restored by treatment with LY294002, a PI3 kinase inhibitor. Moreover, transfection of constitutively active FoxO1 (C/A-FoxO1) restored the insulin-induced suppression of IRS-2. These data suggest that hyperinsulinemia may lead to a decrease of IRS-2-PI3kinase-Akt pathway in the endothelial cells in mouse models of obesity (Fig. 2).

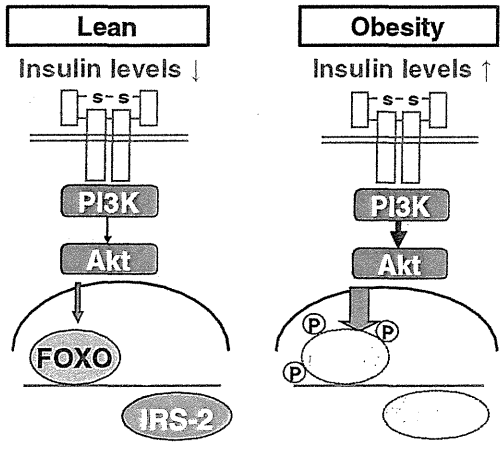

Fig. 2 Hyperinsulinemia is one of the mechanisms underlying the decrease in the expression of endothelial IRS-2 in obesity. In lean subject, expression levels of IRS-2 increased through FoxO1 activation. In contrast, hyperinsulinemia observed in obesity is reduced IRS-2 expression through PI3kinase-Akt-FoxO1 pathway in the endothelial cells

4 Insulin delivery to skeletal muscle is the rate-limiting step in insulin-induced glucose uptake by the skeletal muscle

Insulin, secreted by pancreatic β cells, has to be delivered to skeletal muscle to ensure a supply of insulin to myocytes. Using the compartmental model in the 1970s, Andres and colleagues indicated that insulin was distributed more slowly to the compartment 3 corresponding to skeletal muscle than to other compartments, such as plasma and liver, and that the time-course of insulin equilibration with this pool closely paralleled the glucose infusion rate [41, 42]. Furthermore, the dynamics of insulin concentrations in the skeletal muscle lymphatics, which was derived from the interstitial fluid in the skeletal muscle, was actually slow, and was significantly correlated with the peripheral glucose uptake after insulin infusion [14]. On the other hand, injection of insulin directly into the interstitium of the skeletal muscle was followed by a prompt increase in glucose uptake [43]. It showed a strong correlation between the interstitial insulin concentration and the increase in the glucose uptake by the skeletal muscle.

Moreover, in obese and type 2 diabetes subjects, although insulin distribution to the plasma and liver did not differ significantly, that of skeletal muscle was significantly impaired, and insulin-induced glucose uptake was further delayed in the skeletal muscle as compared with normal subjects [44, 45]. Consistent with these findings, in obese subjects, the appearance and concentrations of insulin in the interstitial fluid of the skeletal muscle were found to be significantly delayed and decreased as compared with control subjects [46]. These findings indicate that insulin delivery to the skeletal muscle is the rate-limiting step in the insulin-induced glucose uptake (Fig. 3). Two discrete steps have been reported for the mechanism regulating insulin delivery to the skeletal muscle: an increase in the trans-endothelial transport of insulin and an increase in the available capillary surface area (capillary recruitment).

5 Insulin delivery to the skeletal muscle

5.1 Trans-endothelial transport of insulin

There is a difference between the types of capillaries in the liver and those in the skeletal muscle. It is thought that the occluded junctions of the endothelial cells of the capillaries in the skeletal muscle may prevent paracellular transport of most macromolecules, including insulin, whereas the fenestrated endothelium of the capillaries in the liver freely permits paracellular passage of macromolecules [47]. In fact, a more rapid insulin action kinetics has been observed in the liver than in the skeletal muscle [16].

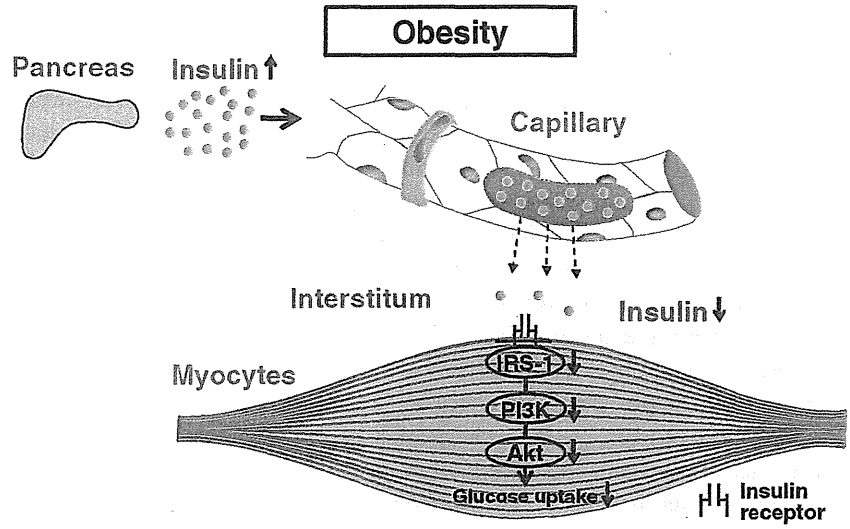

Fig. 3 Insulin delivery to the skeletal muscle is the rate-limiting step in the insulin-induced glucose uptake. The appearance and concentrations of insulin in the interstitial fluid of the skeletal muscle is significantly delayed and decreased in obesity

What mechanisms are involved in trans-endothelial transport of continuous capillaries? There are two different pathways: insulin receptor mediated and non-insulin receptor mediated. King and Johnson reported that the trans-endothelial movement of insulin was saturable in the cultured endothelial cells. This movement was blocked by antibodies against the insulin receptor [48]. Some studies subsequently supported these data *in vitro* [49, 50]. These findings suggest that movement of insulin across the endothelial cells, at least *in vitro*, is insulin receptor-mediated.

In addition to the insulin receptor-mediated pathway, Bergman and colleagues reported that when physiological and pharmacological (very high) levels of insulin were injected into dogs, the steady-state plasma/interstitium gradient was reduced more markedly at the pharmacological rather than physiological insulin level [51]. Moreover, the appearance of the insulin analogue NN304 in dog skeletal muscle interstitial fluid was constant even when sufficient insulin was injected to saturate the endothelial insulin receptors [52]. These data suggest that movement of insulin into skeletal muscle interstitium *in vivo* may partly occur via a non-saturable process such as passive diffusion via a paracellular or transcellular pathway.

Barrett and colleagues measured the rate of ^{125}I-insulin uptake by rat hindlimb muscle for an extremely short period of time (5 min), when unlabelled insulin was infused continuously by hyperinsulinemic-uglycemic clamp. The unlabelled insulin significantly reduced the clearance of ^{125}I-insulin in plasma after 5 min [53, 54]. This observation suggests that the transendothelial movement of insulin is involved in insulin receptor-mediated pathway *in vivo*. Moreover, they noted that when fluorescent-tagged insulin was injected into the rat, the insulin receptor and caveolae were colocalized [55]. Since caveolae had already been implicated in the transcytosis of albumin and other proteins, Wang et al. investigated *in vitro* whether caveolin-1 is required for the transendothelial transport of insulin. Knockdown of caveolin-1 reduced FITC-insulin uptake in bovine aortic endothelial cells. Furthermore, IL-6 or tumour necrosis factor (TNF)α inhibited FITC-insulin uptake as well as the expression of caveolin-1 mRNA and protein [56]. However, systemic caveolae knockout mice showed increased passive diffusion via a paracellular or transcellular pathway [57]. It is still unclear whether insulin receptor-mediated and non-insulin receptor-mediated pathways may be related to each other or may function independently in the physiological and pathophysiological states *in vivo*. A great deal more work needs to be done in order to understand the regulation of this process.

5.2 Insulin regulates capillary recruitment

In 1997, Rattigan and colleagues first showed direct evidence for insulin-mediated capillary recruitment by using 1-methylxathine (1-MX) [58], which has no vasoactivity and is converted solely to 1-methylurate by xanthine oxidase. Xanthine oxidase exists primarily in the endothelial cells of capillaries, but not large vessels [59]. Therefore, 1-MX provides an effective tool for determining capillary recruitment. Using this method, they demonstrated that insulin increased both 1-MX metabolism and glucose uptake in rat hindlimb. However, the clearance of 1-MX by human capillaries is lower than in the rodent, presumably because of lower content of xanthine oxidase [54, 60]. This method could not be adapted to human studies. Barrett and colleagues adapted a contrast enhanced ultrasound (CEU) method that had been extensively used in cardiac muscle [61, 62]. Using this technique, they found that capillary recruitment was significantly enhanced within 30 min of insulin infusion, and this was of similar magnitude to the changes observed at 90 min. On the other hand, an increase of blood flow was observed 120 min after insulin infusion [63]. These data